

**Level crossing analysis of chemically induced dynamic nuclear polarization:
Towards a common description of liquid-state and solid-state cases**

Denis V. Sosnovsky, Gunnar Jeschke, Jörg Matysik, Hans-Martin Vieth, and Konstantin L. Ivanov

Citation: *The Journal of Chemical Physics* **144**, 144202 (2016); doi: 10.1063/1.4945341

View online: <http://dx.doi.org/10.1063/1.4945341>

View Table of Contents: <http://scitation.aip.org/content/aip/journal/jcp/144/14?ver=pdfcov>

Published by the [AIP Publishing](#)

Articles you may be interested in

[Broadband cross-polarization-based heteronuclear dipolar recoupling for structural and dynamic NMR studies of rigid and soft solids](#)

J. Chem. Phys. **144**, 034201 (2016); 10.1063/1.4939798

[Numerical simulation of free evolution in solid-state nuclear magnetic resonance using low-order correlations in Liouville space](#)

J. Chem. Phys. **133**, 224501 (2010); 10.1063/1.3505455

[Theoretical and experimental studies of chemically induced dynamic nuclear polarization kinetics in recombination of radical pairs by the method of switched external magnetic field. II. \$^{13}\text{C}\$ CIDNP of micellized radical pairs](#)

J. Chem. Phys. **111**, 5491 (1999); 10.1063/1.479862

[Analyses of the local order in poly\(ethylene terephthalate\) in the glassy state by two-dimensional solid-state \$^{13}\text{C}\$ spin diffusion nuclear magnetic resonance spectroscopy](#)

J. Chem. Phys. **109**, 4651 (1998); 10.1063/1.477070

[Theoretical and experimental studies of CIDNP kinetics in recombination of radical pairs by the method of switched external magnetic field. I. Theory](#)

J. Chem. Phys. **107**, 9942 (1997); 10.1063/1.475297



NEW Special Topic Sections

NOW ONLINE
Lithium Niobate Properties and Applications:
Reviews of Emerging Trends

AIP | Applied Physics
Reviews

Level crossing analysis of chemically induced dynamic nuclear polarization: Towards a common description of liquid-state and solid-state cases

Denis V. Sosnovsky,^{1,2} Gunnar Jeschke,³ Jörg Matysik,⁴ Hans-Martin Vieth,^{1,5}
 and Konstantin L. Ivanov^{1,2,a)}

¹*International Tomography Centre of SB RAS, Institutskaya 3a, 630090, Novosibirsk, Russia*

²*Novosibirsk State University, Pirogova 2, 630090, Novosibirsk, Russia*

³*Institut für Physikalische Chemie, ETH Zürich, Vladimir-Prelog-Weg 2, CH-8093 Zürich, Switzerland*

⁴*Institut für Analytische Chemie, Universität Leipzig, Linnéstr. 3, D-04103 Leipzig, Germany*

⁵*Institut für Experimentalphysik, Freie Universität Berlin, Arnimallee 14, D-14195 Berlin, Germany*

(Received 8 February 2016; accepted 21 March 2016; published online 14 April 2016)

Chemically Induced Dynamic Nuclear Polarization (CIDNP) is an efficient method of creating non-equilibrium polarization of nuclear spins by using chemical reactions, which have radical pairs as intermediates. The CIDNP effect originates from (i) electron spin-selective recombination of radical pairs and (ii) the dependence of the inter-system crossing rate in radical pairs on the state of magnetic nuclei. The CIDNP effect can be investigated by using Nuclear Magnetic Resonance (NMR) methods. The gain from CIDNP is then two-fold: it allows one to obtain considerable amplification of NMR signals; in addition, it provides a very useful tool for investigating elusive radicals and radical pairs. While the mechanisms of the CIDNP effect in liquids are well established and understood, detailed analysis of solid-state CIDNP mechanisms still remains challenging; likewise a common theoretical frame for the description of CIDNP in both solids and liquids is missing. Difficulties in understanding the spin dynamics that lead to the CIDNP effect in the solid-state case are caused by the anisotropy of spin interactions, which increase the complexity of spin evolution. In this work, we propose to analyze CIDNP in terms of level crossing phenomena, namely, to attribute features in the CIDNP magnetic field dependence to Level Crossings (LCs) and Level Anti-Crossings (LACs) in a radical pair. This approach allows one to describe liquid-state CIDNP; the same holds for the solid-state case where anisotropic interactions play a significant role in CIDNP formation. In solids, features arise predominantly from LACs, since in most cases anisotropic couplings result in perturbations, which turn LCs into LACs. We have interpreted the CIDNP mechanisms in terms of the LC/LAC concept. This consideration allows one to find analytical expressions for a wide magnetic field range, where several different mechanisms are operative; furthermore, the LAC description gives a way to determine CIDNP sign rules. Thus, LCs/LACs provide a consistent description of CIDNP in both liquids and solids with the prospect of exploiting it for the analysis of short-lived radicals and for optimizing the polarization level. © 2016 AIP Publishing LLC. [<http://dx.doi.org/10.1063/1.4945341>]

I. INTRODUCTION

Chemically Induced Dynamic Nuclear Polarization (CIDNP) is a method of creating non-equilibrium polarization of nuclear spins by using chemical reactions, having radical pair (RP) intermediates. The CIDNP effect can be explained using the Radical Pair Model (RPM): polarization originates from (i) electron spin-selective recombination of radical pairs and (ii) the dependence of the singlet-triplet Inter-System Crossing (ISC) rate in RPs on the state of magnetic nuclei.¹ Thus, nuclear “spin sorting” takes place meaning that the RP reactivity depends on its nuclear spin state. As a result, the reaction product is enriched (or depleted) in particular nuclear spin states, i.e., its nuclear spins become non-thermally polarized. The CIDNP effect can be investigated by using Nuclear Magnetic Resonance (NMR) methods. The gain from CIDNP is twofold: first, it allows one to obtain considerable

enhancement of NMR signals and second, CIDNP is a very useful tool for investigating elusive radicals and radical pairs, which are often beyond the reach of Electron Paramagnetic Resonance (EPR) spectroscopy. Nuclear influence on the electron spin evolution originates from electron-nuclear interactions in RPs, i.e., from hyperfine interactions, playing the key role in CIDNP formation. Accordingly, CIDNP effects become pronounced only when the electron-nuclear spin evolution has enough time to develop, i.e., when these interactions (when measured in frequency units) are greater than or comparable to the reciprocal of the RP lifetime.

While the mechanisms of the CIDNP effect in liquids are well established and understood, CIDNP mechanisms in the solid state are not yet fully clear. Differences between solid-state (ss) and liquid-state (ls) CIDNP are due to the following reasons. First, in solids RPs can be long-lived, since the molecular mobility is restricted and the radicals cannot diffuse apart. In this situation, all RPs would eventually recombine independent of their nuclear spin state; consequently, the RP recombination reaction would not work as a nuclear “spin

^{a)} Author to whom correspondence should be addressed. Electronic mail: ivanov@tomo.nsc.ru. Tel.: +7(383)330-8868. Fax: +7(383)333-1399.

sorting” mechanism; hence, enrichment of the product with particular nuclear spin states is not possible. However, the same problem also exists in the liquid state when rigid or flexible biradicals are used: in this situation CIDNP can be formed due to (i) nuclear spin relaxation in the paramagnetic state (i.e., in an RP or biradical), (ii) the presence of an additional spin-independent channel of RP decay (scavenging), or (iii) by the $S-T_{\pm}$ mechanism (to be introduced below). The second factor, which makes the two cases different, is the anisotropy of electron-nuclear spin interactions in solids, which is averaged out in liquids. It is important to note that such interactions change the spin dynamics and open additional pathways for ISC in RPs. More generally, in magnetic resonance, they give rise to new effects; striking examples of such kind are electron spin echo envelope modulation,² solid-effect,^{3,4} and cross-effect⁵⁻⁷ Dynamic Nuclear Polarization (DNP), and EPR-detected NMR.⁸

Theoretical consideration of the effects of such interactions is challenging, because additional couplings render spin evolution more complex.⁹ Up to now, several ss-CIDNP mechanisms have been proposed, which are termed Differential Decay (DD),¹⁰ Differential Relaxation (DR),¹¹⁻¹³ and Three-Spin Mixing (TSM).^{14,15} However, the complete analysis of ss-CIDNP is still a challenging theoretical problem: since polarization is formed due to the spin dynamics in RPs, which undergo spin-selective recombination, CIDNP represents a complex interplay between spin dynamics and reaction dynamics. For this reason, analytical considerations of ss-CIDNP are limited. Furthermore, there is until now no general view on ss-CIDNP and ls-CIDNP: so far both situations are treated rather separately, despite being just two versions of the same general CIDNP technique. The problem of theoretical consideration of ss-CIDNP is further complicated by a rather limited number of systems, which exhibit polarization: in contrast to liquids, where there is a vast number of suitable experimental systems, in solids CIDNP remains limited to photosynthetic reaction centers¹⁶ and flavoproteins.¹⁷ Interestingly, however, all natural photosynthetic reaction centers investigated have been demonstrated to show the effect.^{18,19} Presently, flavoproteins represent the only system, where both ls-CIDNP²⁰⁻²³ and ss-CIDNP^{17,24} have been observed (even then, for slightly different flavoproteins).

In this work we aim at bridging the existing gaps in understanding CIDNP. Specifically, our goal is to find a reasonably simple description of CIDNP, which is valid in solids and in liquids, and to provide a general concept of ss-CIDNP. In particular, we focus on the analytical treatment of CIDNP and aim to derive ss-CIDNP sign rules. Finally, we try to come up with a comprehensive description of CIDNP, which is valid in liquids and in solids. Thus, we propose to look at ss-CIDNP from a more general perspective, avoiding the presentation of different special cases as separate CIDNP mechanisms (i.e., DD, DR, and TSM). In this contribution we only deal with coherent mechanisms of polarization transfer but do not cover the less efficient relaxation based pathways, also known as triplet mechanism of CIDNP.²⁵

To reach the goals of our work we exploit the following key idea: all features in the dependence of CIDNP on the

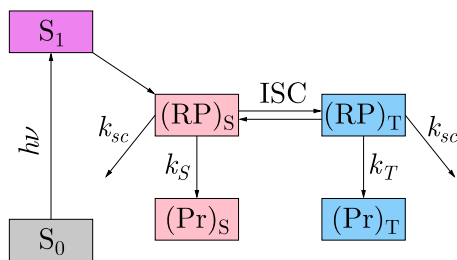
external magnetic field (no matter whether in solids or in liquids) can be associated with particular crossings or avoided crossings of the spin energy levels in RPs. Therefore, the problem is reduced to mapping out Level Crossings (LCs) and avoided crossings, also termed Level Anti-Crossings (LACs), of an RP; their positions immediately yield the matching conditions, i.e., the magnetic field where the corresponding feature is found. When we know which particular levels have an LC or an LAC, we can also determine the type of spin mixing and derive CIDNP sign rules. In general, CIDNP formed by the “spin sorting” mechanism originates from (i) electron-spin selective recombination and (ii) different ISC rates in different nuclear sub-ensembles, i.e., from competition between such sub-ensembles. We demonstrate below that due to LCs/LACs there is always a particular sub-ensemble, which wins (or loses) in this competition resulting in CIDNP formation. Additionally, as also shown below, LACs can promote transfer of the electron spin order of an RP (e.g., singlet spin order) to nuclear spins. The reason why we use this approach is that previously it has been demonstrated that the description based on LACs is very useful for unraveling the otherwise complex dynamics of nuclear spin systems with non-thermal polarization.²⁶⁻²⁹ It is also known that in optical nuclear polarization, a technique related to CIDNP, LACs play an important role and determine the magnetic field strengths where polarization can be transferred from electron spins to nuclear spins.³⁰⁻³² Recently, it has been demonstrated³³⁻³⁵ that in solid-state DNP experiments under magic-angle spinning (MAS), the electron-nuclear polarization transfer is also due to LACs. Such LACs occur upon sample spinning allowing to fulfill certain matching conditions for orientation-dependent interactions. In fact, spin dynamics at such LACs provides the dominant contribution in MAS-DNP experiments. The concept of allowed and avoided crossings of levels is also well known from optics,^{36,37} chemical kinetics (e.g., in electron transfer reactions,³⁸ proton transfer,³⁹ and proton-coupled electron transfer⁴⁰) and photochemistry.⁴¹

In this work, we first test that our approach is valid; the test study is done for ls-CIDNP, which is presently well understood. We demonstrate here that all ls-CIDNP features can be interpreted in terms of LCs and LACs. The same holds for the solid-state case with its anisotropic interactions. In solids, features arise usually from LACs (and almost never from LCs), since the additional anisotropic couplings always result in perturbations, which turn LCs into LACs. We interpret the known CIDNP mechanisms in terms of the LAC concept and formulate the sign rules for ss-CIDNP for various cases. Besides this, kinetic traces of CIDNP are calculated revealing contributions of different pathways in CIDNP formation. Finally, we present a discussion of CIDNP mechanisms in view of our present understanding.

II. THEORY

A. Reaction scheme

Calculations are performed for the RP reaction presented in Scheme 1. We assume that a singlet RP is formed from a singlet-excited precursor molecule as it is the case in



SCHEME 1. Scheme of RP reactions, which give rise to CIDNP, as considered here. In this example, an RP is generated in the electronic singlet spin state from a singlet-excited precursor, S_1 . The RP can undergo singlet-triplet ISC; the singlet and triplet RPs recombine to products of the same multiplicity, $(Pr)_S$ and $(Pr)_T$, at rates k_S and k_T , respectively. The scavenging process (spin-independent RP decay) is also shown; its rate is equal to k_{sc} .

photosynthetic systems. The RP undergoes ISC between the singlet and triplet states; here we consider only coherent spin evolution and neglect relaxation-induced transitions. The RP recombines from the singlet and triplet states at rates k_S and k_T , respectively, to reaction products of the same multiplicity. Generally, these rates are different: $k_S \neq k_T$. We also consider spin-independent decay of RPs, i.e., RP scavenging. In liquids, this can also be diffusional separation of the RPs. The scavenging rate is denoted as k_{sc} . Unless otherwise stated, we consider an RP with one magnetic spin-1/2 nucleus having a hyperfine coupling (HFC) with the electron of radical 1. Denoting the radicals as “radical 1” and “radical 2” is of importance because in some cases the sign of CIDNP depends on the sign of the difference in g -factors of the radicals; i.e., the polarization sign is different depending on whether the nucleus is belonging to the radical with smaller (or greater) g -factor.

Spin-correlated RPs^{1,42} can be generated in liquid phase, for instance, by using photo-excitation to create a singlet excited molecule or triplet excited molecule. Upon bond cleavage a pair of radicals can be formed, which has exactly the same spin state as the RP precursor due to the fact that the electron spin (in most cases) is conserved in the elementary event of a chemical reaction. An alternative way to form a spin-correlated RP is given by (i) creating a photo-excited molecule in its singlet or triplet state and (ii) subsequent quenching of the excited molecule by means of electron or H-transfer. This method is used, for instance, in applications of CIDNP to biologically relevant molecules.⁴³ In both cases the RP inherits the spin state of the precursor molecules. In this work, when discussing Is-CIDNP, we deal only with “geminate” RPs, i.e., RPs born in the same elementary chemical event. Such RPs can recombine (in most cases from the electron singlet state) or avoid recombination due to diffusional separation of the radicals. Radicals escaping recombination can react in the solvent bulk with radicals coming from other RPs. Such bulk recombination can also give rise to CIDNP and strongly affects the time dependence of polarization.^{44,45} However, for the sake of simplicity and clarity, this contribution to the overall polarization is not considered here.

Is-CIDNP can also be formed in biradicals, formed in a particular spin state after photo-excitation. A typical example is given by flexible biradicals formed after photo-excitation of cyclic ketones.^{46–49} Spin-selective recombination of such

biradicals gives rise to pronounced CIDNP. In this case, the radical centers cannot separate by diffusion; also electron-electron interaction is significant. However, spin interaction tensors are completely averaged to their isotropic parts, i.e., the spin Hamiltonian of the RP is the Hamiltonian valid for isotropic liquids. In some matrices, namely, in those pertaining molecular mobility in the solid phase, ss-CIDNP can be formed. Previous studies^{50–52} show that such ss-CIDNP behaves qualitatively similar to Is-CIDNP, i.e., due to the residual molecular mobility only isotropic spin interactions are responsible for CIDNP formation. There are also literature examples of CIDNP with rigid biradicals.^{53,54}

In solids, spin-correlated RPs can be formed by intramolecular electron transfer after photo-excitation. A striking example is given by RPs formed in photosynthetic reaction centers.¹⁶ In flavo-proteins (mutated in order to remove a cysteine residue next to the chromophore), it is also possible to form a spin-correlated RP. Such RPs recombine, generally speaking, from both singlet and triplet states, giving rise to strong ss-CIDNP. Because of the rigid environment, molecular mobility is strongly restricted; therefore, anisotropic spin interactions come into play and affect the evolution of the RP.

It is also important to emphasize that CIDNP formation is often accompanied by magnetic field effects on chemical reactions. For instance, the yield of the reaction product originating from RPs recombining from their singlet state depends on the rate of singlet-triplet conversion. In turn, the conversion rate depends on the external magnetic field. By monitoring the reaction yield as a function of the external magnetic field strength one can measure so-called MARY (Magnetically Affected Reaction Yield) curves, which exhibit features corresponding to LCs and LACs in the RP under investigation. Theoretical analysis of such curves allows one to probe magnetic interactions in short-lived RPs. There is a close similarity between MARY curves and CIDNP magnetic field dependences: both phenomena indirectly probe the RP spin dynamics, the difference is only in the observable, which is either the reaction yield (in MARY) or spin polarization of the diamagnetic reaction product (in CIDNP). The relation between CIDNP and MARY is discussed below, as well as the role of LCs and LACs therein.

B. LCs and LACs

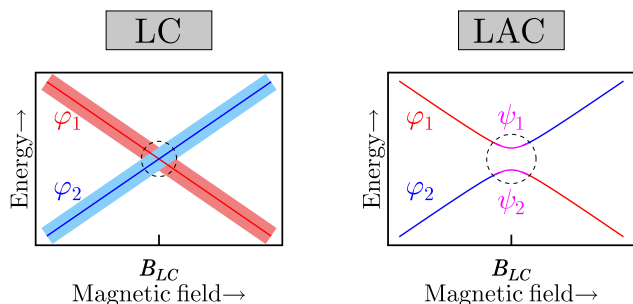
Before going into detail of the theoretical treatment we would like to explain what are an LC and an LAC. Both cases are schematically described in Scheme 2.

In order to introduce the concepts of LCs and LACs, we split the RP spin Hamiltonian \hat{H} into two terms, its main part \hat{H}_0 and a perturbation \hat{V}

$$\hat{H} = \hat{H}_0 + \hat{V}. \quad (1)$$

Let us now assume that at a certain magnetic field strength, B_{LC} , there is a crossing of two energy levels of \hat{H}_0 . Specifically, we mean that the solution of the eigen-problem of \hat{H}_0 is known

$$\hat{H}_0|\varphi_i\rangle = E_i|\varphi_i\rangle \quad (2)$$



SCHEME 2. Left: Level Crossing (LC); right: Level Anti-Crossing (LAC). Here we assume that at some magnetic field strength, B_{LC} , two energy levels of the main Hamiltonian \hat{H}_0 cross, corresponding to spin states $|\varphi_1\rangle$ and $|\varphi_2\rangle$. If there is no coupling matrix element $V_{12} = 0$, the LC will not be perturbed. If the RP preparation is such that it generates a coherence ρ_{12} between the states, this coherence stops evolving at the LC point. In the discussion of LC effects, we take into account the fact that levels are lifetime broadened, i.e., they have finite width, as schematically shown in the left plot. If the matrix element V_{12} is non-zero the LC turns into an LAC: the crossing is avoided (the minimal splitting is $2V_{12}$). At the LAC region the eigen-states of the full Hamiltonian are no longer $|\varphi_1\rangle$ and $|\varphi_2\rangle$, but their linear combinations $|\psi_1\rangle$ and $|\psi_2\rangle$. See text for further explanation.

and that $E_1(B_{LC}) = E_2(B_{LC})$. If the corresponding matrix element of the perturbation, $V_{12} = \langle \varphi_1 | \hat{V} | \varphi_2 \rangle$, is zero the energies, E_1 and E_2 , and wave-functions, $|\varphi_1\rangle$ and $|\varphi_2\rangle$, stay unperturbed, see Scheme 2 (left). Such LCs can be important for CIDNP for the following reason. When an RP is generated in a particular electron spin state, see explanation above, not only the populations of different states, given by the diagonal matrix elements of the RP density matrix ρ_{ii} , are different from each other but there are also spin coherences formed, given by the off-diagonal matrix elements ρ_{ij} . The reason for this is that the initial RP state is not necessarily an eigen-state of its spin Hamiltonian. A typical example is given by an RP formed in the electron singlet state at high magnetic fields,¹ i.e., when the eigen-states of the Hamiltonian are not the singlet-triplet states but the Zeeman states, $[\alpha\alpha, \alpha\beta, \beta\alpha, \beta\beta]$ (hereafter, the spin-up and spin-down states are denoted by α and β , respectively). In this situation, the RP density matrix at $t = 0$ is equal to $\rho(t = 0) = |S\rangle\langle S|$. In the Zeeman basis its elements are $\rho_{ij} = \langle i | \rho | j \rangle$; after re-calculating the density matrix in this basis (eigen-basis of the Hamiltonian) we obtain the following non-zero elements:

$$\rho_{\alpha\beta, \alpha\beta} = \rho_{\beta\alpha, \beta\alpha} = \frac{1}{2}, \quad \rho_{\alpha\beta, \beta\alpha} = \rho_{\beta\alpha, \alpha\beta} = -\frac{1}{2}. \quad (3)$$

Thus, non-zero off-diagonal elements (coherences) are formed, i.e., a singlet-born RP is formed in a coherent superposition of true eigen-states of the Hamiltonian. One should note that in this case the diagonal elements (populations) of the electronic eigen-states $\alpha\beta$ and $\beta\alpha$ are equal to each other; consequently, spin evolution of the RP is due to the coherences between these states, termed Zero-Quantum Coherences (ZQCs). Indeed, the time dependence of each element of the density matrix is as follows:

$$\rho_{ij}(t) = \rho_{ij}(t = 0) \exp\left(-\frac{i}{\hbar}(E_i - E_j)t\right). \quad (4)$$

Thus, the eigen-state populations do not evolve at all, whereas the coherences oscillate at the frequency given by

the difference in energies of the corresponding states. In an RP, the evolution of the $\rho_{\alpha\beta, \beta\alpha}$ and $\rho_{\beta\alpha, \alpha\beta}$ coherences, i.e., ZQCs, is responsible for singlet-triplet mixing. Indeed, the singlet state population changes with time in the following way:

$$\rho_{SS}(t) = \langle S | \rho(t) | S \rangle = \frac{1 + \cos(\Delta E t / \hbar)}{2}, \quad (5)$$

where $\Delta E = (E_{\alpha\beta} - E_{\beta\alpha})$. Hence, the singlet-state population oscillates at a frequency $\Delta E / \hbar$ between 1 and 0, i.e., coherent singlet-triplet transitions are occurring. The coherent evolution is thus driven by the ZQCs.

When there is an LC (this happens when there is a matching of the difference in the electronic Zeeman interactions and hyperfine interactions with nuclear spins, see below) the frequency $\Delta E / \hbar$ becomes zero and ISC is turned off in a particular nuclear spin ensemble. As a consequence of nuclear spin sorting, this results in a peak in the CIDNP field dependence. Below, we demonstrate how this effect reveals itself in CIDNP.

When $V_{12} \neq 0$, we obtain a different kind of behavior: the levels never cross, i.e., the LC is “avoided” and turns into an LAC, see Scheme 2 (right). Thus, instead of the LC point, we obtain an LAC region; the minimal splitting between the levels becomes equal to $2V_{12}$, when $V_{11} = V_{22} = 0$ the splitting is minimal exactly at $B = B_{LC}$ (otherwise, it can shift from B_{LC} but the minimal splitting is always $2V_{12}$). What is very important is that LACs have a strong effect on the type of spin mixing and on the spin mixing efficiency. This is because at an LAC the eigen-states of the full Hamiltonian, \hat{H} , differ from those of \hat{H}_0 . Specifically, for the given pair of levels having an LAC, the new eigen-states are

$$\begin{aligned} |\psi_1\rangle &= \cos \theta |\varphi_1\rangle + \sin \theta |\varphi_2\rangle, \\ |\psi_2\rangle &= -\sin \theta |\varphi_1\rangle + \cos \theta |\varphi_2\rangle. \end{aligned} \quad (6)$$

At the center of the LAC region the “mixing angle” is $\theta = \pm\pi/4$ so that the true eigen-states differ drastically from the pure $|\varphi_1\rangle$ and $|\varphi_2\rangle$ states: as the states become mixed, the spin evolution of the RP changes. Below we demonstrate LC/LAC effects in Is-CIDNP and then show how LCs turn into LACs in the ss-CIDNP case and modify the spin evolution.

Finally, in this subsection we discuss the magnetic field range, in which LC/LAC effects are operative. At first glance, LC has a “zero” width, i.e., it occurs at a single point. However, one should bear in mind that due to the finite RP lifetime the energy levels are broadened (as follows from the time uncertainty principle). For this reason, the LC point is spread and the LC “width” is determined by the inverse RP lifetime. This point is addressed below in detail. The LAC “width” is given by the field range where the matrix element V_{12} is greater than or comparable to the splitting of the corresponding levels of \hat{H}_0 . In this range the states φ_1 and φ_2 are mixed considerably, see Eq. (6), and the RP spin evolution is altered. However, when the RP decay rate becomes comparable to V_{12} the LAC becomes lifetime broadened, just as well as an LC does.

One should also note that the situation of a pure LC is, probably, never met in practice because any small perturbation would turn this LC into an LAC. However, when the LC

“width” is greater than the width of such an LAC region, it is legitimate to talk about a pure LC effect.

We can also deduce the characteristic time scale, on which the LC/LAC effects become pronounced. LCs are of importance when the lifetime broadening of energy levels matches their splitting. LAC effects become pronounced when the mixing term, V_{12} , is (at least) comparable to the reciprocal of the RP lifetime.

Thus, LCs/LACs selectively slow down or promote specific spin mixing. In turn, this either affects nuclear “spin sorting” or induces specific nuclear spin flips; both effects result in CIDNP formation.

C. Calculation method

To perform calculations of CIDNP we solve numerically the stochastic Liouville equation for the spin density matrix of the RP. In this equation we take into account coherent spin evolution in the RP, which is described by the Hamiltonian \hat{H} , see below, and also RP reactivity. We assume that the RP reacts to form a polarized product from its singlet and triplet states at rates k_S and k_T , respectively; generally, $k_S \neq k_T$. In addition, we assume a reaction channel, which leads to RP decay independent of its spin state. This decay channel can be considered as RP scavenging, which occurs due to side-reactions of radicals. In parallel to the nuclear-spin dependent ISC there is another pathway induced by spin-orbit coupling. As a consequence, the RP can change its spin multiplicity without involvement of the nuclear spin. This pathway is of particular importance when heavy atom nuclei are present in radicals;⁴⁷ for the sake of simplicity, it is neglected in the present description.

When Is-CIDNP is considered the “scavenging” channel mainly corresponds to diffusional separation of RPs. For simplicity, this additional decay is characterized by a rate k_{sc} (in the case of diffusion such a treatment may be an oversimplification, but here we do not treat such details); the scavenging time is defined as $1/k_{sc}$.

The stochastic Liouville equation for the RP density matrix is as follows (when the energies are expressed as angular frequencies, i.e., $\hbar = 1$):

$$\frac{d\rho}{dt} = -i[\hat{H}, \rho] - \frac{k_S}{2} \{\hat{P}_S, \rho\} - \frac{k_T}{2} \{\hat{P}_T, \rho\} - k_{sc} \rho \quad (7)$$

The coherent dynamics is accounted for by the commutator term; spin-selective reactions are described by the anti-commutator terms with \hat{P}_S and \hat{P}_T being the projection operators on the RP singlet and triplet states, respectively; the additional reaction channel is considered as a mono-exponential decay at a rate k_{sc} . The initial condition for this equation is $\rho(t=0) = \rho_0$; the ρ_0 matrix describes a singlet-born or triplet-born RP, i.e., $\rho_0 = z\hat{P}_S$ or $\rho_0 = z\hat{P}_T$ (with z being a coefficient providing correct normalization, $\text{Tr}\{\rho_0\} = 1$). This normalization is used throughout the paper. For the sake of clarity, we always assume here that the RP is singlet-born. The stochastic Liouville equation is solved numerically to calculate CIDNP.

One should note that the trace of ρ is equal to unity only at $t = 0$ because RPs decay with time, as described by the last

three terms in Eq. (7). Normalization of the trace is possible when the RP along with all reaction products are taken into account, i.e., the product of the singlet-state and triplet-state reactions, as well as the product of “scavenging”: the sum of the traces of the corresponding density matrix is indeed equal to 1 at any instant of time. In general, consideration of all the pathways is of importance in CIDNP. For instance, in liquids RPs, which avoid spin-selective recombination, carry strong polarization that is equal in size but opposite in sign to CIDNP formed after recombination of the geminate RP. Consideration of this polarization is very important for quantitative analysis of the CIDNP time dependence.^{44,45}

Polarization of the reaction product is calculated as follows:

$$P = \langle I_z \rangle = \langle I_z \rangle_S + \langle I_z \rangle_T. \quad (8)$$

Thus, as we assume $\text{Tr}\{\rho_0\} = 1$, the calculated CIDNP is always polarization per one RP that has reacted. Hereafter, for simplicity, we ignore polarization of the products of “scavenging.” However, we can differentiate CIDNP of the singlet reaction product, $\langle I_z \rangle_S$, and of the triplet reaction product, $\langle I_z \rangle_T$, and calculate separately the two contributions to polarization,

$$\begin{aligned} \langle I_z \rangle_S(t) &= \text{Tr} \left\{ \hat{I}_z \cdot k_S \int_0^t \hat{P}_S \rho(\tau) d\tau \right\}, \\ \langle I_z \rangle_T(t) &= \text{Tr} \left\{ \hat{I}_z \cdot k_T \int_0^t \hat{P}_T \rho(\tau) d\tau \right\}. \end{aligned} \quad (9)$$

As usual, polarization is given by the expectation value of the \hat{I}_z spin operator; the rate of polarization formation via the two channels is given by the density matrices $k_S \hat{P}_S \rho(\tau)$ and $k_T \hat{P}_T \rho(\tau)$. For calculating the steady-state polarization we perform integration from $\tau = 0$ to ∞ ; when the CIDNP kinetics is of interest, the upper limit for integration is set to t .

To solve the stochastic Liouville equation we use the following procedure. The general solution of this equation is written as follows:

$$\begin{aligned} \rho(t) &= \exp(-k_{sc}t) \exp\left(-i\hat{H}t - \frac{k_S}{2}\hat{P}_St - \frac{k_T}{2}\hat{P}_Tt\right) \\ &\times \rho(0) \exp\left(i\hat{H}t - \frac{k_S}{2}\hat{P}_St - \frac{k_T}{2}\hat{P}_Tt\right) \\ &= \exp(-k_{sc}t) \exp(-\hat{A}_+t) \rho(0) \exp(-\hat{A}_-t). \end{aligned} \quad (10)$$

To calculate the matrix exponentials we first diagonalize each of the matrices \hat{A}_\pm

$$\hat{A}_\pm = \pm i\hat{H} + \frac{k_S}{2}\hat{P}_S + \frac{k_T}{2}\hat{P}_T \quad (11)$$

and obtain their eigen-values, L_i^\pm , and matrices of eigen-vectors, \hat{T}^\pm

$$\hat{\Lambda}^\pm = \{\hat{T}^\pm\}^{-1} \hat{A}_\pm \hat{T}^\pm, \text{ where } \Lambda_{ij}^\pm = \delta_{ij} L_i^\pm, \quad (12)$$

with δ_{ij} being the Kronecker delta. This allows us to calculate the matrix exponents in Eq. (10) and to perform integration

over time. As a result we obtain

$$\int_0^t \rho_{ij}(\tau) d\tau = \sum T_{ik}^+ T_{lk}^+ \rho_{lm}(0) T_{mn}^- T_{jn}^- \times \frac{1 - \exp((k_{sc} + \Lambda_{kk}^+ + \Lambda_{nn}^-)t)}{k_{sc} + \Lambda_{kk}^+ + \Lambda_{nn}^-}. \quad (13)$$

Integration from 0 to ∞ gives the following result:

$$\int_0^{\infty} \rho_{ij}(t) dt = \sum T_{ik}^+ T_{lk}^+ \rho_{lm}(0) T_{mn}^- T_{jn}^- \frac{1}{k_{sc} + \Lambda_{kk}^+ + \Lambda_{nn}^-}. \quad (14)$$

After that the numerical solution is reduced to linear algebraic operations with matrices: we multiply the density matrix with the elements given by Eq. (14) with \hat{P}_S (or \hat{P}_T) and \hat{I}_z and take the trace to obtain CIDNP. This solution method avoids numerical integration over time. The method can be used to calculate both steady-state and time-dependent CIDNP.

When results for different cases are presented we start with a CIDNP field dependence and then show the RP energy levels highlighting the relevant LCs/LACs. Energy levels are always shown for manifolds of selected electron-nuclear spin states where the LCs/LACs are occurring. Thus, we present numerical results and then interpret them in terms of LCs/LACs to get physical insight into the underlying spin evolution. In some cases, namely, for ss-CIDNP we also show an energy level diagram corresponding to the situation where a specific LAC is encountered in order to give a clear description of the spin dynamics.

In our calculations, we assume magnetic parameters, which are typical for organic radicals. Specifically, differences in the g -factors of RP partners are of the order of 10^{-3} ; HFC constants are of the order of 1 mT (which is typical for protons); electronic spin-spin interactions are varied in the range from 0 to 100 mT. The reaction rates are varied up to values of about 1 ns^{-1} .

III. RESULTS

First, we consider ls-CIDNP, which is well understood by now, to demonstrate the validity of our approach. Then we perform a similar LC/LAC analysis in the solid-state case.

A. Liquid-state CIDNP

In the case where only isotropic spin interactions are present, we just reproduce well-known results in order to demonstrate that they can be interpreted using the level-crossing analysis. Once anisotropic interactions come into play we discuss different CIDNP mechanisms. Description of each mechanism starts with the energy level diagram and discussion of relevant LCs and LACs, continues with the calculation of the CIDNP field dependence and ends with a derivation of CIDNP sign rules.

Let us describe the role of LCs and LACs in the ls-case; we do so separately for the two cases of zero and non-zero electron-electron exchange coupling. In the case of an isotropic

liquid the dipolar coupling of the electron spins is averaged out to zero; hence, it is always omitted in this subsection. Likewise, in the exchange coupling we take only its isotropic part, J_{ex} .

1. Isotropic case, $J_{ex} = 0$

First, for simplicity, we neglect the electron-electron exchange coupling J_{ex} . This means that the radicals do not interact with each other, i.e., in the RP Hamiltonian they are independent from each other. However, the absence of such interaction does not mean that the radicals evolve independently: due to the RP preparation in a spin-correlated state there is a ZQC formed. As already mentioned, its evolution is of great importance for CIDNP. When $J_{ex} = 0$ the Hamiltonian of a three-spin system (two electrons and one nucleus) at a magnetic field B_0 can be written as (in \hbar units)

$$\begin{aligned} \hat{H} &= g_1 \mu_B B_0 \hat{S}_{1z} + g_2 \mu_B B_0 \hat{S}_{2z} - g_N \mu_N B_0 \hat{I}_z + a (\hat{\mathbf{S}}_1 \cdot \hat{\mathbf{I}}) \\ &= \omega_1 \hat{S}_{1z} + \omega_2 \hat{S}_{2z} - \omega_N \hat{I}_z + a (\hat{\mathbf{S}}_1 \cdot \hat{\mathbf{I}}). \end{aligned} \quad (15)$$

Here a is the isotropic HFC constant, $g_{1,2}$ are the g -factors of radicals 1 and 2; hereafter, we prefer to specify all Zeeman interactions in angular frequency units, i.e., later in the text, we use the notations: $\omega_N = g_N \mu_N B_0$, $\omega_{1,2} = g_{1,2} \mu_B B_0$, and $\Delta\omega_e = (g_1 - g_2) \mu_B B_0 = \Delta g \mu_B B_0$ (with μ_B being the Bohr magneton and μ_N being the nuclear magneton). Hereafter, the electronic spin operators are denoted as \hat{S}_1 and \hat{S}_2 ; the nuclear spin operator is denoted as \hat{I} ; $\hat{\mathbf{F}}$ stands for the operator of the total spin, i.e., $\hat{\mathbf{F}} = \hat{\mathbf{S}}_1 + \hat{\mathbf{S}}_2 + \hat{\mathbf{I}}$. To specify eigen-states of the spin Hamiltonian we use the Zeeman basis of states (i.e., electron spins have well-defined projections and their states are denoted as $|\alpha\rangle$ or $|\beta\rangle$) or the singlet-triplet basis,

$$\begin{aligned} |T_+\rangle &= |\alpha\alpha\rangle, |T_0\rangle = \frac{|\alpha\beta\rangle + |\beta\alpha\rangle}{\sqrt{2}}, |T_-\rangle = |\beta\beta\rangle, \\ |S\rangle &= \frac{|\alpha\beta\rangle - |\beta\alpha\rangle}{\sqrt{2}}. \end{aligned} \quad (16)$$

The nuclear spin states are characterized by the z -projection of the nuclear spin; the nuclear spin-up and spin-down states are denoted as $|\alpha_N\rangle$ and $|\beta_N\rangle$, respectively.

In the case under consideration, there is a good correlation between the LC/LAC positions and the features in the field dependence of CIDNP, see Figures 1 and 2. The maximum in the high-field CIDNP (at $B_{LC} = a/2\beta\Delta g$) is due to an LC between the $\alpha\beta\alpha_N$ and $\beta\alpha\alpha_N$ levels, see Figure 1, the low-field feature (at a field approximately equal to a) in the field dependence is an effect of two LACs, occurring at zero field in two different spin manifolds (Figure 2). In Figure 1 one can see an additional LC between the $\alpha\beta\alpha_N$ and $\alpha\beta\beta_N$ levels (at a field where the HFC term matches the nuclear Zeeman term); however, this LC does not contribute to ls-CIDNP because the coherence between the corresponding states (differing by the projection of the nuclear spin) is zero. In solids, however, this LC becomes important, see below.

The high-field LC affects CIDNP for the following reason. When the RP is singlet-born, there are not only populations of the $\alpha\beta\alpha_N$ and $\beta\alpha\alpha_N$ levels but also the coherence between them. After RP formation, this coherence starts to oscillate resulting in S- T_0 electronic transitions, i.e., singlet-triplet

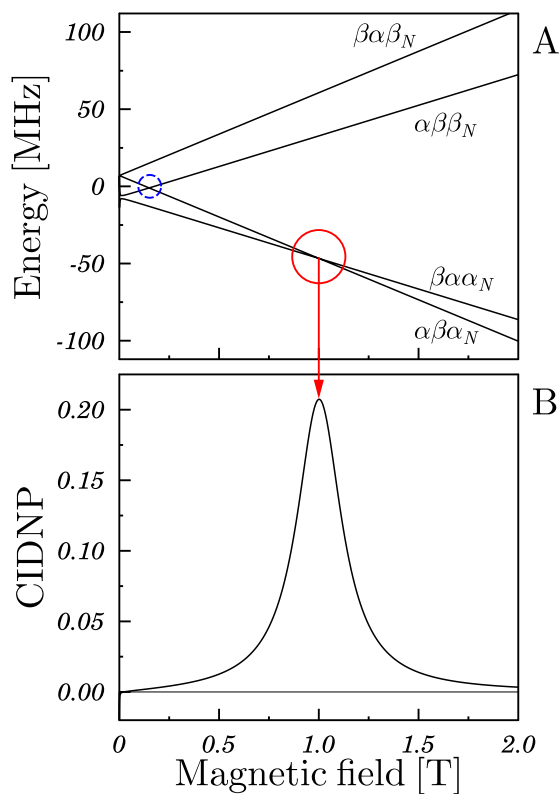


FIG. 1. Field dependence of the energy levels (a) of radical pair with one nucleus (manifold of states characterized with zero z -projection of the electron spin is shown) and CIDNP (b) at high fields. The feature in the CIDNP field dependence corresponds to the crossing of the levels corresponding to states $|\alpha\beta\alpha_N\rangle$ and $|\beta\alpha\alpha_N\rangle$; another LC does not result in a feature in the field dependence, see text for explanation. The relevant LC is highlighted. Parameters used in calculation: $g_1 = 2$ and $g_2 = 2.001$ are the electronic g -factors; the nucleus is a proton; $a = 1$ mT is the hyperfine interaction constant; exchange coupling is zero; $k_S = k_T = 0.01$ ns $^{-1}$, $k_{sc} = 0.02$ ns $^{-1}$ is the scavenging rate. Here in (b) we show only polarization formed in the product of singlet-state recombination; the calculated CIDNP is polarization per RP.

conversion in the RP.¹ The frequency of the oscillations is proportional to the splitting between the corresponding levels, therefore, it is zero at the LC point. For this reason, a particular channel of singlet-triplet conversion, corresponding to a particular nuclear spin state (in our case, the α_N state) is turned off. Consequently, the RP reactivity in this nuclear spin state becomes higher (for a singlet-born RP and $k_S > k_T$) resulting in a feature in the CIDNP field dependence. At the same time, the other LC does not lead to CIDNP formation because the coherence is zero between the corresponding states, $\alpha\beta\alpha_N$ and $\alpha\beta\beta_N$, since these states have different z -projections of the nuclear spin, i.e., they belong to different nuclear spin ensembles, which are not mixed.

The sign of polarization, hereafter denoted as Γ , at high fields is^{1,55}

$$\Gamma = \text{sgn}(\Delta g) \times \text{sgn}(a) \times \mu. \quad (17)$$

Hereafter, μ is determined by the spin state of the RP precursor

$$\mu = \begin{cases} 1, & \text{T-precursor} \\ -1, & \text{S-precursor} \end{cases} \quad (18)$$

Indeed, when the sign of Δg and a is different, we obtain an LC of the levels $\alpha\beta\alpha_N$ and $\beta\alpha\alpha_N$. This means that in the α_N

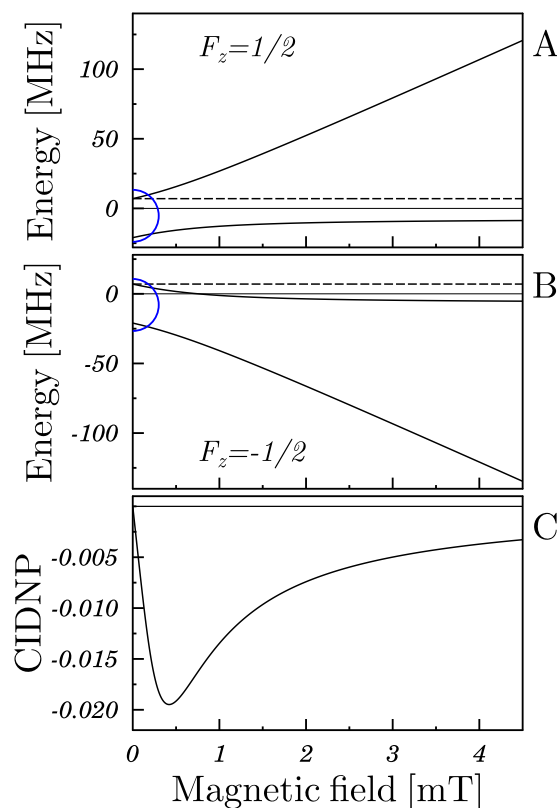


FIG. 2. Field dependence of the energy levels (a) and (b) of radical pair (RP) with one nucleus and CIDNP (c) at low magnetic fields. The feature in CIDNP comes from the two overlapping LACs shown in the figure marked with semi-circles; levels having LACs are shown by solid lines; the other levels are shown by dashed lines. Parameters used in calculation: $a = 1$ mT is the hyperfine interaction constant; exchange coupling is zero; $k_S = k_T = 0.01$ ns $^{-1}$, $k_{sc} = 0.02$ ns $^{-1}$. In (a) and (b) we present the states characterized by $F_z = \frac{1}{2}$ and $F_z = -\frac{1}{2}$, respectively. Here in (c) we show only polarization formed in the product of singlet-state recombination; the calculated CIDNP is polarization per RP.

state S-T conversion is slowed down; therefore, in the case of a singlet-born RP this state is enriched in the reaction product and CIDNP is positive. Upon sign inversion of Δg or a the sign of CIDNP changes, as well as when the RP is triplet-born (i.e., when μ changes sign). This simple consideration is consistent with Eq. (17).

The LAC effect is different. At an LAC, there is efficient mixing of the levels, which would tend to cross in the absence of coupling, i.e., the eigen-states of the Hamiltonian change significantly. In our simple example, the RP with only one magnetic nucleus has an LAC at zero magnetic field. This LAC occurs in radical 1. Indeed, in the absence of the coupling term (namely, non-secular HFC), there is a crossing of levels $\alpha\beta_N$ and $\beta\alpha_N$ of radical 1. The coupling term mixes them making an LAC out of the LC and the new states become a superposition of the old states. In the presence of the second radical we obtain two LACs, i.e., the same LAC is found for the α -state and β -state of the second electron, namely, LACs between $\alpha\alpha\beta_N = T_+\beta_N$ and $\beta\alpha\alpha_N$ and between $\alpha\beta\beta_N$ and $\beta\beta\alpha_N = T_-\alpha_N$ (compare Figures 2(a) and 2(b)). At $t = 0$ the $T_+\beta_N$ and $T_-\alpha_N$ have zero population, but the other two states, $\beta\alpha\alpha_N$ and $\alpha\beta\beta_N$, having singlet character are populated. To explain in detail how these LACs

work it is necessary to add into consideration also the states $\alpha\beta\alpha_N$ and $\beta\alpha\beta_N$, which have singlet character and are involved in spin mixing. The reason for this is that in a singlet-born RP at $t = 0$ there is a coherence, specifically, ZQC, between the states $\alpha\beta\alpha_N$ and $\beta\alpha\alpha_N$ and also between $\alpha\beta\beta_N$ and $\beta\alpha\beta_N$. In general, since the z -projection of all three spins is conserved, spin mixing is occurring separately in two ensembles, $[T_+\beta_N, \alpha\beta\alpha_N, \beta\alpha\alpha_N]$ (all these states are characterized by $F_z = \frac{1}{2}$) and $[T_-\alpha_N, \alpha\beta\beta_N, \beta\alpha\beta_N]$ (all these states are characterized by $F_z = -\frac{1}{2}$); in each ensemble there is an interplay of the $S \leftrightarrow T_0$ mixing (as described above) and $S \leftrightarrow T_{\pm}$ mixing at LACs. At a non-zero field the coherences of interest evolve at a different frequency because the spacing between the corresponding pairs of levels is different: in our example, it is smaller for $\alpha\beta\alpha_N$ and $\beta\alpha\alpha_N$ (compare Figures 2(a) and 2(b)). Consequently, the transitions to the $T_+\beta_N$ states become less efficient than the transitions to the $T_-\alpha_N$ state and negative CIDNP is found in the case of a singlet-born RP,^{1,56} see Figure 2(c).

To provide further insight into the RP spin dynamics we calculate the reaction yield arising from the two ensembles with $F_z = \pm\frac{1}{2}$, see Figure 3. In both cases, there is a sharp maximum of the yield at zero field, which originates from an LC at zero field. These LCs are of great importance for

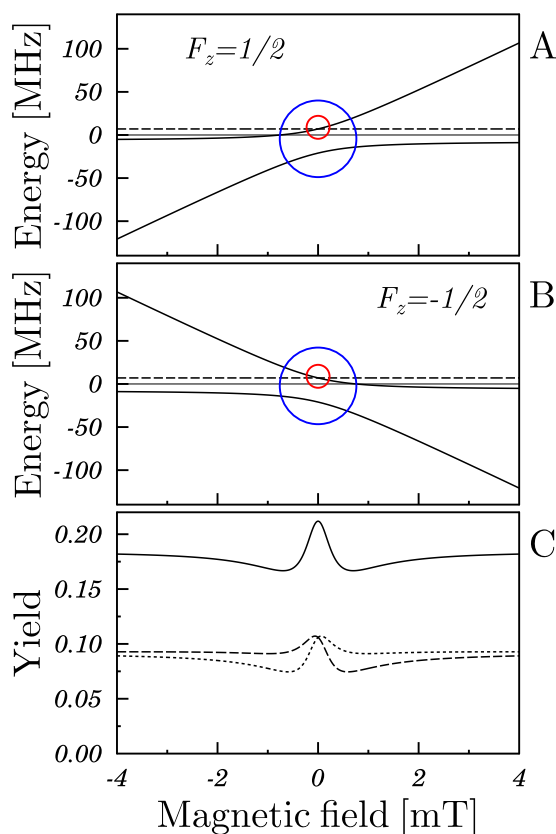


FIG. 3. Field dependence of the energy levels (a) and (b) of radical pair (RP) with one nucleus and RP recombination yield (c) at low magnetic fields. In (a) and (b) we present the states characterized by $F_z = \frac{1}{2}$ and $F_z = -\frac{1}{2}$, respectively; LACs and LCs are marked by circles. Parameters used in the calculation are the same as those in Figure 2. Here in (c) we show the reaction yield for the $F_z = \frac{1}{2}$ states (dashed line), $F_z = -\frac{1}{2}$ states (dotted line) and the total yield (solid line). Here the yield of singlet-state RP recombination (per RP) is shown.

MARY spectroscopy, but they do not manifest themselves in CIDNP because of the different observable. The reason is that at zero magnetic field (i.e., in the absence of a field) there is no preferred axis in space so that the spins cannot be polarized along a particular direction. In addition, there is a broad feature, which shows up only for the $F_z = \frac{1}{2}$ ensemble (for $F_z = -\frac{1}{2}$ such a feature exists at a negative field, which does not have a physical reality). Thus, the RP states with positive F_z are more “reactive”; consequently, the reaction product is enriched in the α_N states of the nuclear spin. The MARY spectrum exhibits at zero field a narrow feature, originating from the LCs, and a broad feature, coming from the LACs.

Upon inversion of the HFC constant CIDNP changes the sign. Thus, at low fields CIDNP obeys the following sign rule:^{1,57}

$$\Gamma = \text{sgn}(a) \times \mu. \quad (19)$$

Features in CIDNP coming from the LC and LAC demonstrate different behavior upon variation of the RP lifetime. The width of the LC-derived features is sensitive to the RP lifetime, equal to $1/k_{sc}$, the width of the LAC-derived feature has a less pronounced dependence on k_{sc} (see the supplementary material,⁵⁸ Figures 1S and 2S). In general, if coherent singlet-triplet mixing in a certain spin ensemble is occurring at a frequency ω and the RP lifetime is $1/k_{sc}$ the contribution of this ensemble to the overall reaction yield is proportional to

$$\int_0^{\infty} \cos(\omega t) e^{-k_{sc} t} dt = \frac{1/k_{sc}}{1 + (\omega/k_{sc})^2}. \quad (20)$$

Thus, each LC produces (on top of a smooth background) a peak of the width k_{sc} in the MARY curves and CIDNP (except for the zero-field LC, which is manifest only in the MARY curve). The dependence of the LC-derived feature on the RP lifetime is very well-known in spin chemistry: the field dependence of the RP recombination yield exhibits sharp peaks originating from LCs.^{59–62} In our case the dependence on relevant RP parameters is more complex, but the general behavior is the same. The width of the feature coming from an LAC is determined by the actual width of the LAC region and does not depend strongly on k_{sc} .

In the discussion of the LC-derived feature we would also like to stress three more points.

First of all, one should note that in practice LCs are rarely met because almost any perturbation, which mixes the crossing levels, will turn the LC into an LAC. Such an interaction could be, for instance, a residual electron-electron coupling, which is, generally, non-zero and can manifest itself once the solvent viscosity is high enough. In this situation, one should compare the width of the corresponding LAC region (almost independent of k_{sc} , when $V_{12} > k_{sc}, k_S, k_T$) and the width of the LC-derived feature in the CIDNP field dependence (strongly depending on k_{sc}). When the latter is considerably larger, the effects of the residual interactions can be neglected and one can assume that CIDNP is due to a pure LC effect. However, in the opposite case the LC consideration must be revised and this additional coupling must be taken into account.

The second important point is that the LC-derived feature is sensitive not only to k_{sc} but also to the distribution of the RP lifetimes. In this work we assume that the “scavenging” process is described by a simple mono-exponential decay of RPs; however, this is not true when the spin-correlated RPs decay due to diffusional separation, which is typical for Is-CIDNP. Previous MARY studies have revealed that not only the width of LC-derived features is sensitive to k_{sc} but that their shape also reflects the distribution of RP lifetimes.⁶³ In supplementary material, we demonstrate that similar effects are expected for Is-CIDNP: comparison of the diffusional model and the exponential model show quite a different behavior (the calculation of CIDNP is done using the same method as described in Refs. 64 and 65). Notably, in the case of diffusional motion of radicals the LC-derived feature is sharp (formally, the derivative of the field dependence, CIDNP(B), is not existing at this point), whereas for the exponential model it is smooth, compare Figures 1 and 3S.

Third, one should note that any process (for instance, spin relaxation) resulting in the decay of the S- T_0 coherence in an RP would lead to an analogous effect as a decreased RP lifetime does. Such a behavior is well-understood in the MARY case^{66–68} and it is expected for CIDNP as well. However, a detailed discussion of spin relaxation effects⁶⁹ is beyond the scope of this work.

2. Isotropic case, $J_{ex} \neq 0$

Now let us add the electron-electron interaction into consideration. In this case the Hamiltonian for the spin system is written as

$$\hat{H}_0 = g_1 \mu_B B_0 \hat{S}_{1z} + g_2 \mu_B B_0 \hat{S}_{2z} - g_N \mu_N B_0 \hat{J}_z + a (\hat{\mathbf{S}}_1 \cdot \hat{\mathbf{I}}) - J_{ex} \left[2 (\hat{\mathbf{S}}_1 \cdot \hat{\mathbf{S}}_2) + \frac{1}{2} \right]. \quad (21)$$

In the presence of exchange interaction between the electron spins one more feature appears at a field where the electron Zeeman interaction equals twice the exchange coupling, $2|J_{ex}|$.¹ At this field, there is a crossing of the S and T_{\pm} levels: in the case of positive J_{ex} we obtain the S - T_+ crossing, when $J_{ex} < 0$ the levels, which cross, are S and T_- . Non-secular HFC is known to induce transitions, which conserve the z -projection of the total spin, i.e., $S\alpha_N \leftrightarrow T_+\beta_N$ and $S\beta_N \leftrightarrow T_-\alpha_N$ converting the corresponding LCs into LACs. Since these transitions are selective with respect to the nuclear spin state, CIDNP is formed at such LACs, see Figure 4. The width of the feature coming from such an LAC depends only slightly on the RP lifetime, $1/k_{sc}$ (in the chosen range of parameters, i.e., the coupling matrix element given by the HFC term is large). Interestingly, the sign of polarization does not depend on the sign of HFC: CIDNP is determined by the type of the LAC, i.e., $S\alpha_N \leftrightarrow T_+\beta_N$ or $S\beta_N \leftrightarrow T_-\alpha_N$. In the former case (for the singlet RP precursor) we obtain negative CIDNP, in the latter case nuclear polarization is positive. Consequently, we arrive at the well-known sign rule for the S- T_{\pm} mechanism¹

$$\Gamma = \text{sgn}(J_{ex}) \times \mu. \quad (22)$$

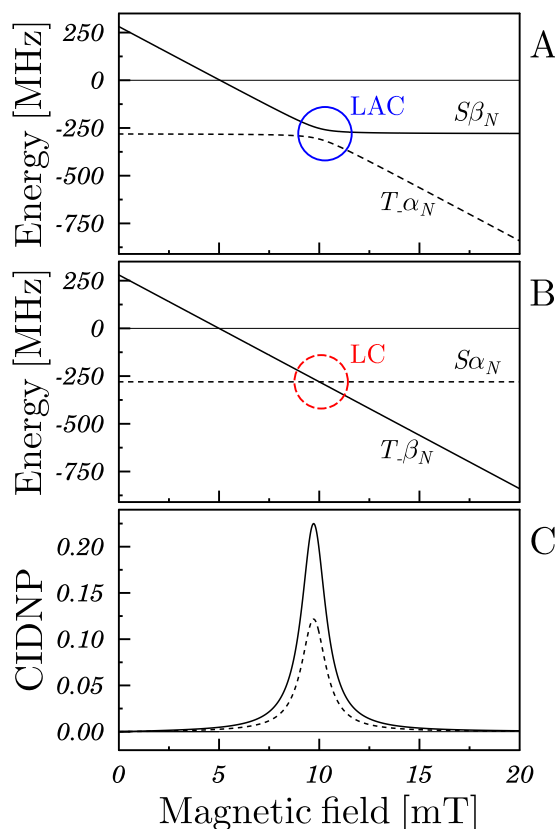


FIG. 4. Field dependence of the energy levels (a) and (b) and CIDNP (c). The feature in the CIDNP field dependence corresponds to the LAC at $B_0 \sim 2|J|$. Parameters used in calculation: $g_1 = 2$ and $g_2 = 2.001$ are the electronic g -factors; the nucleus is a proton; $a = 1$ mT; $J_{ex} = -5$ mT is the exchange electron-electron coupling; $k_S = k_T = 0.01$ ns⁻¹, $k_{sc} = 0.01$ ns⁻¹ (dashed line), 0.001 ns⁻¹ (solid line). In (a) and (b) we compare pairs of levels with an LAC and LC; the corresponding states are indicated. Here in (c) we show only polarization formed in the product of singlet-state recombination; the calculated CIDNP is polarization per RP.

Thus, the polarization sign depends only on the spin multiplicity of the precursor and on the sign of the exchange coupling, J_{ex} . One should note, that J_{ex} is rarely constant because of the molecular mobility; therefore, our results allow only for a qualitative account of CIDNP in the presence of the electron-electron exchange interaction. When J_{ex} depends on time, the calculation scheme has to be revised, as done, for instance, by de Kanter *et al.*⁴⁷ The RP spin dynamics also changes: the RP spin system does not remain statically at the relevant LAC at $\omega_e = 2|J_{ex}|$ but passes through this LAC as J_{ex} changes with time. However, the behavior of CIDNP remains qualitatively the same: polarization formation is an LAC effect and the CIDNP sign is accounted for by Eq. (22). Moreover, in many cases an effective average J_{ex} value is introduced, which is time-independent rendering the Hamiltonian time-independent as well. Detailed discussion of the validity of such an approximation is beyond the scope of this work and is not discussed here.

Hence, we have demonstrated that in the Is case the features in the CIDNP field dependence can be interpreted in terms of LCs and LACs. Furthermore, by using the level crossing description the sign rules for CIDNP can be derived, which are fully consistent with the known rules. Now let

us apply the same procedure to solid-state CIDNP, a case where anisotropic interactions play a significant role and spin dynamics becomes by far more complex. It is of interest and importance to find out what interactions are essential for CIDNP formation in the solid state and to interpret the results in terms of LCs and LACs. In solids, we expect that the features will mostly come from LACs, since anisotropic couplings usually result in perturbations, which turn all LCs into LACs.

B. Solid-state CIDNP

Thus, let us focus our attention on studying mechanisms of CIDNP formation in solids in the presence of anisotropic couplings. Here, we consider in detail the case of *high external magnetic fields*. By high fields we mean that the electron Zeeman interaction is much greater than both HFC and the electron-electron coupling. Detailed considerations of the more complex low-field case⁷⁰ are beyond the scope of the present work.

In solids, the RP Hamiltonian for a system of two electrons and a spin- $1/2$ nucleus coupled to electron 1 is written as follows:

$$\hat{H} = g_{1,zz}\mu_B B_0 \hat{S}_{1z} + g_{2,zz}\mu_B B_0 \hat{S}_{2z} - g_N \mu_N B_0 \hat{I}_z + \hat{\mathbf{S}}_1 \mathbf{A} \hat{\mathbf{I}} - J_{ex} \left[2(\hat{\mathbf{S}}_1 \cdot \hat{\mathbf{S}}_2) + \frac{1}{2} \right] + \hat{\mathbf{S}}_1 \mathbf{D} \hat{\mathbf{S}}_2. \quad (23)$$

Here $g_{1,zz}$ and $g_{2,zz}$ are the zz -components of the corresponding g -tensors (hereafter, for brevity we use shorthand notations: $g_1 = g_{1,zz}$, $g_2 = g_{2,zz}$); \mathbf{A} is the HFC tensor, \mathbf{D} is the electron-electron dipolar interaction tensor. At high magnetic fields, the Hamiltonian can be simplified. First, in the HFC tensor we keep only the secular part, $A_{zz}\hat{S}_{1z}\hat{I}_z + a\hat{S}_{1z}\hat{I}_z$, and the pseudo-secular part, $A_{zx}\hat{S}_{1z}\hat{I}_x + A_{zy}\hat{S}_{1z}\hat{I}_y$. The secular HFC comprising the dipolar and scalar interactions is hereafter written as $A\hat{S}_{1z}\hat{I}_z$. The pseudo-secular HFC can be simplified by rotating the frame so that the hyperfine field component in the xy plane of the laboratory frame defines the new x axis.⁷¹ After such a rotation the pseudo-secular term becomes equal to $b\hat{S}_{1z}\hat{I}_x$ with $b = \sqrt{A_{zx}^2 + A_{zy}^2}$. In the dipolar and exchange interaction we will keep only the secular part, $\hat{S}_{1z}\hat{S}_{2z}$, and the non-secular part, $(\hat{S}_{1+}\hat{S}_{2-} + \hat{S}_{1-}\hat{S}_{2+})$. Thus, the dipolar terms containing only a single raising or lowering operator are neglected, as well as the terms containing $\hat{S}_{1+}\hat{S}_{2+}$ and $\hat{S}_{1-}\hat{S}_{2-}$. Specifically, the non-secular part of both interactions combined together will be written as $d(\hat{S}_{1+}\hat{S}_{2-} + \hat{S}_{1-}\hat{S}_{2+})$ with $d = -2J_{ex} - D$ and with D being the dipole-dipole interaction strength. In Eq. (23) we exclude the anisotropic part of the exchange coupling; when needed, this interaction can be added as well; at high field, only the secular and non-secular parts of the interaction tensor should be considered. In the high-field approximation electronic spin mixing is possible only between the singlet and T_0 states, since the S - T_{\pm} transitions become energy forbidden. In this situation, the secular interaction gives the same additive contribution to energies of all states in the S - T_0 manifold and can be omitted in the analysis of high-field polarization.

In solids, CIDNP studies are usually performed under magic angle spinning of the sample, which is a prerequisite for high-resolution NMR detection. Upon spinning, the magnetic interactions introduced here change with time. However, in calculations of CIDNP the time dependence of the parameters entering Eq. (23) can be safely neglected, since the typical RP recombination rates are much greater than achievable sample spinning frequencies. Thus, on the time scale of RP recombination, the spin interactions can be treated as time-independent.

In our numerical analysis we keep all terms in the general Hamiltonian. The high-field case splits into two different cases: (i) zero electron-electron coupling, corresponding to the DD and DR mechanisms (ii) non-zero coupling, corresponding to the TSM case.

1. DD/DR mechanisms

A calculated CIDNP field dependence for a typical set of calculation parameters, along with the relevant energy levels, is presented in Figure 5. In this case, there is a single LC and a single LAC, each significantly affecting the RP spin dynamics.

As follows from the energy level diagram shown in Figure 5(a), we have the same LC as in the isotropic case (matching of energies of the $\alpha\beta\alpha_N$ and $\beta\alpha\alpha_N$ states) and an LAC in addition. In the isotropic case, the corresponding pair of levels has an LC coming from matching of the secular

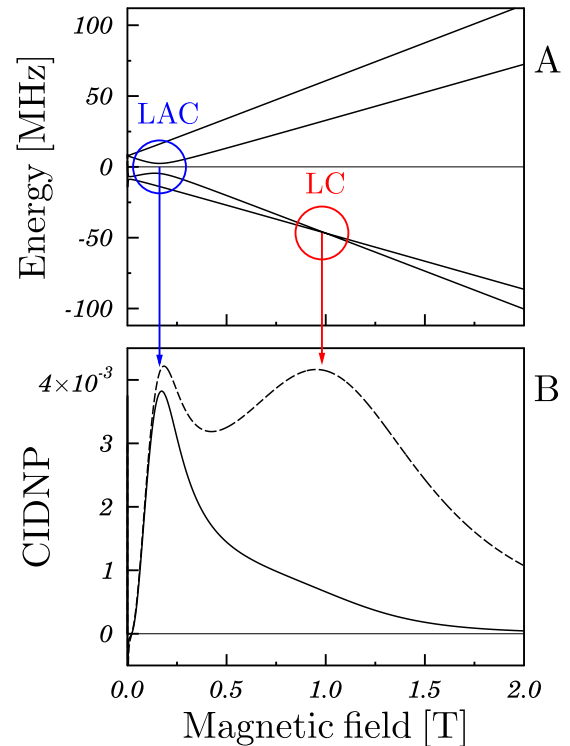


FIG. 5. Field dependence of energy levels (a) and field dependence of CIDNP (b). Parameters used in calculation: $g_1 = 2$ and $g_2 = 2.001$; the nucleus is a proton; $A = 1$ mT; $d = 0$; $k_S = 2k_T = 0.08$ ns $^{-1}$, $b = 0.5$ mT, $k_{sc} = 0.002$ ns $^{-1}$ (dashed line), $k_{sc} = 0$ (solid line); the calculated CIDNP is polarization per RP. In (a) the LAC is highlighted by a blue circle and LC is highlighted by a red circle.

HFC and nuclear Zeeman terms, see Figure 1, which has no effect on CIDNP. However, in the anisotropic case the pseudo-secular HFC mixes the $\alpha\beta\alpha_N$ and $\alpha\beta\beta_N$ states turning the LC into an LAC and enabling nuclear spin flips $\alpha_N \leftrightarrow \beta_N$, compare the behavior of these levels in Figures 1(a) and 5(a). Calculations shown in Figure 5 show that both LC and LAC can contribute to CIDNP; however, the LC contribution to CIDNP completely vanishes when $k_{sc} \rightarrow 0$ (at a very small k_{sc} this feature becomes very narrow). In contrast, the LAC contribution is manifested even at $k_{sc} \rightarrow 0$ when the recombination rates are different, $k_S \neq k_T$. As has been discussed earlier, the difference in rates is a pre-requisite for obtaining CIDNP from this mechanism: when $k_S = k_T$ CIDNP is zero. The RP lifetime also affects the CIDNP amplitude, see Figure 5.

The LAC, which is formed when $|\omega_N| = |A/2|$, works here even despite the fact that the anti-crossing levels start with identical populations; furthermore, there is no coherence between these states in a singlet-born RP. The reason for this is that the LAC affects the S-T₀ conversion rate in pairs of states $\beta\alpha\beta_N - \alpha\beta\beta_N$ and $\beta\alpha\alpha_N - \alpha\beta\alpha_N$ by perturbing the $\alpha\beta\alpha_N$ and $\alpha\beta\beta_N$ states. As a consequence the S-T₀ conversion via the channel $\beta\alpha\beta_N - \alpha\beta\beta_N$ also affects the $\alpha\beta\alpha_N$ state and flips the nuclear spin. The coherence between a pair of eigen-states oscillates at a frequency proportional to the energy gap between the corresponding energy levels (see the energy level diagram in Figure 6), such oscillations are responsible for S-T₀ conversion in the RP. The conversion is faster for the nuclear spins in the β_N -state ($\beta\alpha\beta_N \leftrightarrow \alpha\beta\beta_N$), in addition, the pseudo-secular HFC mixes $\alpha\beta\beta_N$ and $\alpha\beta\alpha_N$ and leads to efficient nuclear spin transitions $\beta_N \rightarrow \alpha_N$. Consequently, CIDNP with positive sign is formed. This effect requires a non-zero Δg -term: otherwise the situation is symmetric with respect to the nuclear spin state and different coherences evolve at the same frequency, see the energy level diagram presented in Figure 6. Chemical reactions are also involved in CIDNP formation, so that the difference in the recombination rates is crucial: $k_S \neq k_T$. When the rates are the same the RP just decays independent of the nuclear spin state and since, in the absence of electron-electron coupling, the spin evolution alone cannot polarize the nuclei, part of the job is

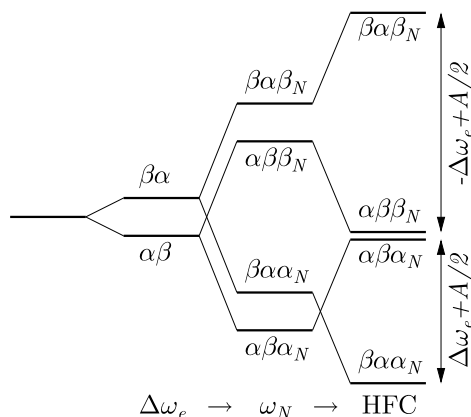


FIG. 6. RP energy levels at the B_{LAC} field (see Figure 5): when $|\omega_N| \approx |A/2|$ the energy levels $\alpha\beta\alpha_N$ and $\alpha\beta\beta_N$ closely approach each other. Here $\Delta g < 0, g_N > 0, A > 0$.

done by reactions. Another way to achieve non-zero CIDNP is to look only at polarization formed in only one of the two RP recombination channels. This is exactly the assumption of the DR-mechanism.

2. Sign rules, DD/DR mechanisms

Assuming that CIDNP is due to state mixing at the LAC, let us now derive the sign rule. Figure 6 shows the RP energy levels. In this particular case, $\Delta g < 0, A > 0, g_N > 0$, the two (central) states, $\alpha\beta\beta_N$ and $\alpha\beta\alpha_N$, are nearly degenerate and have an LAC (when g_N and A have different signs the LAC is occurring for the $\beta\alpha\beta_N$ and $\beta\alpha\alpha_N$ levels). At the same time, the $\beta\alpha\beta_N$ state is more remote from the two central states than the $\beta\alpha\alpha_N$ state, meaning that the corresponding frequency evolves faster. Consequently, the faster S-T₀ conversion channel involves the $\beta_N \rightarrow \alpha_N$ nuclear spin flip, the CIDNP sign is “+” for S-precursor and predominant singlet-state recombination.

Now let us see what happens upon inverting the sign of relevant interactions. Inversion of $\Delta\omega_e$ makes the energy gap between the $\beta\alpha\beta_N$ state and the central states smaller than for the $\beta\alpha\alpha_N$ state causing a change in sign. Inversion of the sign of A has the same effect. When g_N and A have different signs the nearly degenerate levels are the $\beta\alpha\beta_N$ and $\beta\alpha\alpha_N$ levels. In this situation the analysis can be performed in a similar way as previously. The result depends only on the relative signs of Δg and A and does not depend on the signs of ω_N and b (the latter only converts the LC into an LAC but does not affect the type of polarization). Summing everything up, we come to the following sign rule:

$$\Gamma = \text{sgn}(\Delta g) \times \text{sgn}(A) \times \mu \times \psi, \quad (24)$$

where

$$\psi = \begin{cases} 1, & k_S > k_T \\ -1, & k_S < k_T \end{cases}, \text{ for the DD-case,} \quad (25a)$$

$$\psi = \begin{cases} 1, & \text{S-yield} \\ -1, & \text{T-yield} \end{cases}, \text{ for the DR-case.} \quad (25b)$$

Further details concerning the behavior of CIDNP and energy level diagrams for different signs of Δg , A , and g_N are presented in the supplementary material, see Figure 4(S).⁵⁸

3. TSM mechanism

Now let us turn on the electron-electron coupling and assume that the “double matching” condition is fulfilled, which is required in the TSM,^{9,14,15} specifically

$$|\Delta\omega_e| \approx |\omega_N| \approx \frac{|A|}{2}. \quad (26)$$

We also assume that $k_S = k_T$; the discussion of how stringent should be the requirement given by Eq. (26) is presented below.

To perform the LAC analysis we split the Hamiltonian into its main part and perturbation terms

$$\hat{H} = \hat{H}_0 + \hat{H}_{ee} + \hat{H}_b. \quad (27)$$

Here \hat{H}_0 is the main Hamiltonian, $\hat{H}_{ee} = d(\hat{S}_{1+}\hat{S}_{2-} + \hat{S}_{1-}\hat{S}_{2+})$ stands for the non-secular electron-electron coupling and \hat{H}_b is the pseudo-secular HFC term. The main Hamiltonian has the following form:

$$\hat{H}_0 = g_1\mu_B B_0 \hat{S}_{1z} + g_2\mu_B B_0 \hat{S}_{2z} - g_N\mu_N B_0 \hat{I}_z + A\hat{S}_{1z}\hat{I}_z. \quad (28)$$

The first condition $|\Delta\omega_e| = |\omega_N|$ from Eq. (26) results in a degeneracy of the energy levels corresponding to the states $|\beta\alpha\alpha_N\rangle$ and $|\alpha\beta\beta_N\rangle$. The second condition $|\omega_N| = |A/2|$ leads to the degeneracy of energy levels corresponding to the $|\alpha\beta\beta_N\rangle$ and $|\alpha\beta\alpha_N\rangle$ states at a particular magnetic field strength (see the discussion below). To account for CIDNP effects we will take into account the perturbations and see what happens with the energy levels.

The magnetic field dependence of CIDNP in the TSM case is presented in Figure 7. In this field dependence there are two peaks. The low-field one comes from S-T₋ mixing by secular HFC, thus, it has exactly the same nature as that presented in Figure 4. This peak is really a “low-field” feature in the sense that it cannot be reproduced by considering S-T₀ mixing only. Other low-field features are not discussed in this work. The high-field peak arises from S-T₀ mixing occurring due to TSM, see the discussion below.

Let us now have look at the RP energy levels of the system with Hamiltonian \hat{H}_0 at variable magnetic field, see Figure 8, and at the energy level diagram corresponding to the situation of “double matching,” as described by Eq. (26), see Figure 9. When the double matching condition is fulfilled three out of four levels in the S-T₀ manifold become degenerate, see Figure 9, where the energy level $\beta\alpha\alpha_N$ has the same energy as levels $\alpha\beta\beta_N$ and $\alpha\beta\alpha_N$. The fourth state is remote in energy; however, as we see below, it is also involved in the spin dynamics. When a non-zero \hat{H}_{ee} is taken into consideration, the degeneracy between the $\alpha\beta\alpha_N$ and $\beta\alpha\alpha_N$ levels is lifted, so that the LC turns into an LAC: the new eigen-levels become split and the eigen-states become different (this LAC is highlighted in Figure 8). In fact, the behavior of levels corresponds to a triple LAC, i.e., to an “avoided crossing” of three levels. When $d > 0$ the lower state in energy is the $S\alpha_N$ state, while the higher state is $T_0\alpha_N$. Although the other two levels are more remote in energy from each other, the electron-electron coupling has an important

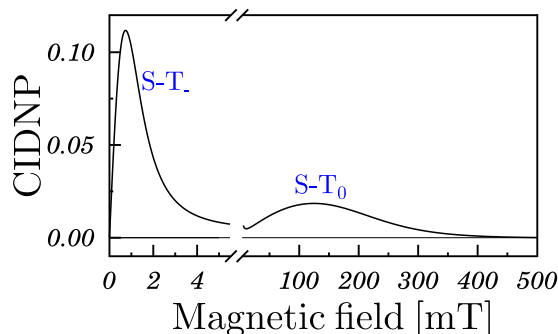


FIG. 7. Field dependence of CIDNP in TSM case. Parameters used in calculation: $g_1 = 2$ and $g_2 = 2.0067$; the nucleus is a proton; $A = 1$ mT; $d = 0.5$ mT; $b = 0.5$ mT, $k_S = k_T = 0.1$ ns⁻¹, $k_{sc} = 0.002$ ns⁻¹; the calculated CIDNP is polarization per RP.

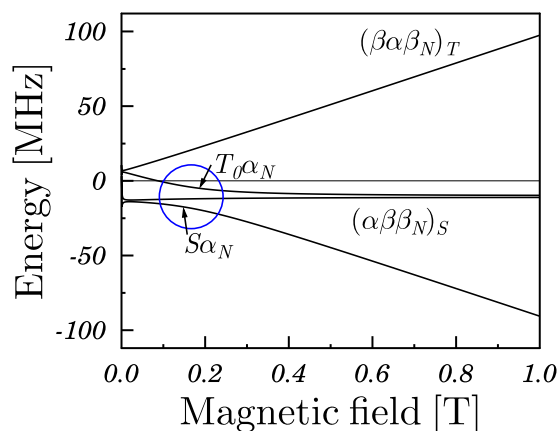


FIG. 8. Field dependence of energy levels in the TSM case; the relevant LAC is indicated. Parameters used in calculation: $g_1 = 2$ and $g_2 = 2.0067$; the nucleus is a proton; $A = 1$ mT; $d = 0.5$ mT; $b = 0$, $k_S = k_T = 0.1$ ns⁻¹, $k_{sc} = 0.002$ ns⁻¹. The notation $(\alpha\beta\beta_N)_S$ means that the corresponding state has S-character higher than $1/2$; $(\alpha\beta\beta_N)_T$ has higher T₀-character; the pseudo-secular HFC is omitted in the calculation to visualize the LAC more clearly.

effect on them as well. Specifically, the lower level is no longer exactly $\alpha\beta\beta_N$ but acquires singlet character higher than $1/2$ for the electron wave-function, likewise, the higher level acquires T₀-character higher than $1/2$ for the electron wave-function; the new states are denoted as $(\alpha\beta\beta_N)_S$ and $(\beta\alpha\beta_N)_T$, respectively. If we take the pure $\alpha\beta\beta_N$ and $\beta\alpha\beta_N$ states (i.e., states far away from an LAC), both of them will have exactly $1/2$ of singlet character (and also $1/2$ of T₀ character). However, in our case this is not exactly true: one of the two states has an admixture of singlet character equal to $(\frac{1}{2} + \delta)$, with $\delta \sim \frac{d}{\Delta E}$ where ΔE is the splitting between the two levels (equal to approximately $2\Delta\omega_e$ when the TSM matching condition, Eq. (26) is imposed); likewise, for the other state the singlet content is $(\frac{1}{2} - \delta)$.

When the RP is singlet-born the $S\alpha_N$ state has a population of $\frac{1}{2}$, the $T_0\alpha_N$ state has zero population, while the other two states, $(\alpha\beta\beta_N)_S$ and $(\beta\alpha\beta_N)_T$, have populations of $(\frac{1}{4} + \frac{\delta}{2})$ and $(\frac{1}{4} - \frac{\delta}{2})$, respectively; here $\delta > 0$ is reflecting the higher S-character for $(\alpha\beta\beta_N)_S$ and the higher T₀-character

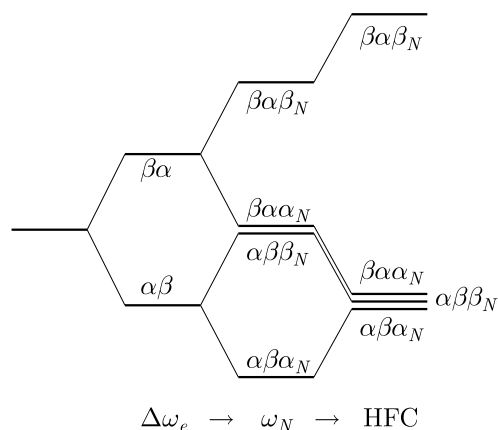


FIG. 9. Schematic representation of energies in the situation where the double matching condition is fulfilled (corresponding to the LAC shown in Figure 8).

for $(\beta\alpha\beta_N)_T$. Thus, the average population of the three nearly degenerate states is equal to $(\frac{1}{4} + \frac{\delta}{6})$, which is higher than $(\frac{1}{4} - \frac{\delta}{4})$ being the population of the $(\beta\alpha\beta_N)_T$ state.

The outlined effect of the electron-electron coupling alone does not produce CIDNP because there are no nuclear spin flips occurring in the system. After taking into account one more perturbation, \hat{H}_b , transitions in the pairs of nearly degenerate states $\frac{\alpha\beta+\beta\alpha}{\sqrt{2}}\alpha_N$ and $(\alpha\beta\beta_N)_S$ as well as $\frac{\alpha\beta-\beta\alpha}{\sqrt{2}}\alpha_N$ and $(\alpha\beta\beta_N)_S$ occur, which mix the state populations flipping the nuclear spin. As a consequence of this mixing, population of the three nearly degenerate states is shared among them. As a result, the RP nuclear state is predominantly α_N and the nuclear spins get polarized. Like in the S-T $_{\pm}$ crossing in the isotropic case, the nucleus is polarized in the same way even when the k_S and k_T rates are arbitrary (although the actual CIDNP amplitude, certainly, depends on these rates). In fact, the spin dynamics in TSM represents a high-field analogue of the S-T $_{\pm}$ spin mixing (although it is operative only in the presence of anisotropic interactions). Indeed, CIDNP is formed due to the evolution of the spin-correlated RP, while the chemical reaction is needed only to transfer this polarization into the final diamagnetic state (which is probed by NMR). Consequently, polarization can be generated even when $k_S = k_T$ and it does not depend on the sign of A , as shown below. The similarity between the two cases is even more salient in the case $\Delta\omega_e = 0$, which is discussed below. For the sake of simplicity, here we do not analyze the dependence of CIDNP on δ ; such an analysis has been performed by numerical calculations in Ref. 9.

The TSM case in CIDNP bears some similarity to the cross-effect DNP,^{5,6} which also requires a matching of energies for a pair of levels, i.e., an LAC of levels $\alpha\beta\alpha_N$ and $\beta\alpha\beta_N$ (or $\alpha\beta\beta_N$ and $\beta\alpha\alpha_N$) occurring when $|\Delta\omega_e| \approx |\omega_N|$. Upon mixing at this LAC, all three spins “flip” and electron spin polarization is transferred to the nucleus.^{7,72} However, the second matching condition is not required in the cross-effect DNP; a further difference between the two cases, CIDNP and cross-effect DNP, comes from the fact that in CIDNP it is required to transfer singlet spin order of the two electrons to the nuclear spins, whereas in DNP electron spin magnetization is transferred to the nuclei. Thus, in TSM-CIDNP not only the degeneracy of the $\alpha\beta\alpha_N$ and $\beta\alpha\beta_N$ (or $\alpha\beta\beta_N$ and $\beta\alpha\alpha_N$) levels is required (i.e., the matching condition $|\Delta\omega_e| \approx |\omega_N|$): there should also be different mixing of these two states with the other two states. This is provided by the non-zero secular HFC, $A \neq 0$. Ideally, Eq. (26) should be fulfilled leading to the triple LAC, see Figure 8. Without this asymmetry, TSM-derived CIDNP is not formed, whereas in cross-effect DNP the second matching condition is not required, moreover, A can be zero.

Before going to the derivation of the CIDNP sign rules, let us discuss how precisely the double matching condition, see Eq. (26), should be fulfilled. In fact, this issue has been investigated before in Ref. 9 by running numerical calculations. Of course, matching between $\Delta\omega_e$ and A (or ω_N and A) can always be achieved by simply varying the external magnetic field strength but the second condition, $\Delta\omega_e = \omega_N$, imposes specific requirements on an RP. However, in a disordered solid, where due to the g -tensor anisotropy

there is a distribution of ω_1 and ω_2 , it might be enough that this requirement is fulfilled only for a fraction of all RPs. A similar situation is typical for cross-effect DNP: only a fraction of all molecular orientations of the paramagnetic polarizing agent is responsible for the observed NMR signal enhancement. Furthermore, Eq. (26) does not mean exact coincidence of the three interactions: numerical calculations rather show⁹ that the three terms, $\Delta\omega_e$, ω_N , and A , should be of the same order of magnitude but that matching or near-matching just two of them is not enough for CIDNP formation.

4. Sign rules, TSM mechanism

As previously, the LAC analysis enables relatively simple assessment of CIDNP sign rules. We have already explained that in the example considered above the CIDNP sign is positive. Let us see what happens upon inversion of sign of relevant interactions.

When the sign of d is inverted, the three nearly degenerate lower states acquire predominantly T₀-character, whereas the higher state predominantly acquires S-character. As a consequence, the CIDNP sign changes.

When the sign of $\Delta\omega_e$ changes, we obtain a different set of nearly degenerate states: $\alpha\beta\beta_N$, $\alpha\beta\alpha_N$, $\beta\alpha\beta_N$, which are higher in energy than the $\beta\alpha\alpha_N$ state. When d is positive (as in the previous case), these states have higher T₀-character but also higher content of the β_N nuclear spin state. As a consequence, CIDNP remains positive. When the sign of A is varied, at positive d we have the same behavior as for inverting the sign of $\Delta\omega_e$: the three nearly degenerate states are $\alpha\beta\beta_N$, $\alpha\beta\alpha_N$, $\beta\alpha\beta_N$, which are higher in energy than the $\beta\alpha\alpha_N$ state. Consequently, they have predominantly T₀-character and the polarization stays positive. Sign inversion of g_N again changes the set of the three nearly degenerate states to $\beta\alpha\alpha_N$, $\beta\alpha\beta_N$, $\alpha\beta\alpha_N$, which are higher in energy than the $\alpha\beta\beta_N$ state. As a consequence, the three nearly degenerate states have predominantly T₀-character, i.e., a lower population, and also higher content of the α_N nuclear spin state. Thus, the polarization sign changes. The pseudo-secular HFC causes only mixing of the three nearly degenerate states. Thus, the sign of CIDNP does not depend on the sign of b . The energy level diagrams for the cases with different sign of the relevant interactions are presented in supplementary material, see Figure 5(S).⁵⁸

Summarizing these considerations, we obtain the following sign rules:

$$\Gamma = -\text{sgn}(d) \times \text{sgn}(g_N) \times \mu. \quad (29)$$

Thus, LACs allow one to obtain the CIDNP sign rule in a rather simple way. Now, with the knowledge that LACs do the job in ss-CIDNP we can *predict* under what conditions we obtain new LACs and different behavior of polarization. Specifically, in the TSM case there can be one more LAC, which occurs when a matching condition different from those given in Eq. (26) is fulfilled

$$|d| = |\omega_N|. \quad (30)$$

Previously, it was mentioned⁹ that the TSM-derived polarization increases when this condition is fulfilled. Here

we show that it indeed corresponds to an LAC in the RP spin system. To make the analysis a bit simpler, let us show how the energy levels are behaving in a situation where $\Delta\omega_e = 0$, such that the singlet-triplet basis is an eigen-basis of the main Hamiltonian, in which the pseudo-secular HFC is omitted. Such a simplification is done only for the sake of clarity, while the conclusions obtained apply to the general Hamiltonian as well.

5. TSM, case of $\Delta g = 0$

Let us consider the TSM case assuming that $\Delta\omega_e = 0$. In this situation, we assume that $g_N > 0$ and $d > 0$; then at a field where $|g_N\mu_N B| = |d|$ (here we put into the calculation a very small secular HFC as compared to ω_N and d) there is an LC of the $|S\beta_N\rangle$ and $|T_0\alpha_N\rangle$ energy levels. The pseudo-secular HFC lifts the degeneracy and mixes the two states. Thus, at this field we obtain an LAC and a peak in the CIDNP field dependence, see Figure 10, because for a singlet-born RP nuclear transitions $\beta_N \rightarrow \alpha_N$ become operative. Like in the general TSM case, the CIDNP sign does not depend on the reaction rates k_S and k_T . As mentioned above, the polarization mechanism bears some similarity to the S- T_{\pm} mechanism in liquids; however, the difference is that the LAC is in the S- T_0 manifold and that the perturbation, which mixes the levels, is due to an anisotropic interaction.

Now let us obtain the sign rule for this type of spin mixing, i.e., let us see what happens upon inversion of the relevant spin interactions.

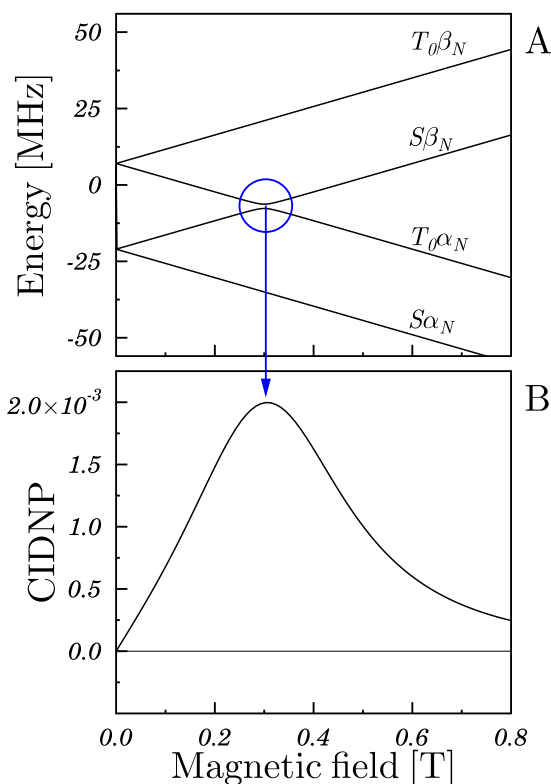


FIG. 10. Field dependence of energy levels (a) and CIDNP (b). Parameters used in calculation: $g_1 = g_2 = 2$; the nucleus is a proton; $A = 0$, $b = 0.1$ mT, $d = 1$ mT; $k_S = k_T = 0.1$ ns $^{-1}$, $k_{sc} = 0.02$ ns $^{-1}$; the calculated CIDNP is polarization per RP.

Upon inversion of the d sign, the pair of degenerate levels becomes $|S\alpha_N\rangle$ and $|T_0\beta_N\rangle$. Then the pseudo-secular HFC works in the same way as before, resulting in nuclear spin flips $\alpha_N \rightarrow \beta_N$, and hence, in a negative CIDNP sign. The same effect is produced by inversion of the sign of g_N . As previously, the result does not depend on the sign of b . Summarizing this discussion, we obtain the sign rule, which is the same as in the previously discussed case, see Eq. (29).

Discussion of the case of $\Delta\omega_e = 0$ is relevant when the RP under study comprises radicals with strongly overlapping EPR spectra, for instance, when the RP contains two identical radicals.

C. ss-CIDNP time dependence

Finally, we would like to emphasize that ss-CIDNP exhibits a rather unusual time dependence. We performed numerical calculations of ss-CIDNP for an RP with two magnetic nuclei having HFCs of opposite sign: $A_1 = -A_2$. CIDNP has been computed for different relative size of k_S, k_T, k_{sc} . In this situation, CIDNP driven by isotropic mechanisms is expected to change its sign according to Kaptein's rule, see Eq. (17); in contrast, the TSM-derived polarization does not depend on the sign of A . Thus, by varying the RP reactivity parameters we can analyze the interplay between the ls-CIDNP and ss-CIDNP mechanisms.

The calculated CIDNP time traces are presented in Figure 11; these time traces demonstrate how different mechanisms come into play.

When the recombination rates are taken unequal, $k_S \neq k_T$, polarization can be formed by the ls-mechanism, see Figure 11(a). However, when $k_{sc} = 0$ at long times CIDNP drops to zero because at $t \rightarrow \infty$ all RPs have decayed independent of their nuclear spin state and, hence, polarization cancels out. When $k_{sc} \neq 0$, see Figure 11(b), this cancellation is incomplete. This situation corresponds to ls-CIDNP: due to diffusional separation of the partner radicals the steady-state polarization is non-zero.

When the two mechanisms are working in a concerted way, the CIDNP time traces change significantly. For instance, see Figure 11(c), at short times CIDNP is consistent with Kaptein's rules, whereas at long times CIDNP of both nuclei is of the same sign as the TSM contribution becomes dominant.

Finally, when $k_S = k_T$ only the TSM contribution is manifest and both nuclei have exactly the same CIDNP time dependence, see Figure 11(d).

Thus, at different times, different mechanisms can become dominant. Therefore, time-resolved ss-CIDNP potentially provides much more information about the RP state than its steady-state analogue.

We also expect that CIDNP can be affected by nuclear spin relaxation in the RPs (relaxation in diamagnetic reaction products is much slower and can be safely neglected). For instance, relaxation, which tends to equilibrate the populations of the α_N and β_N states in transient radicals can result in non-zero steady state polarization even when $b = 0$ and $k_{sc} = 0$. However, consideration of such effects is not along the lines of this contribution.

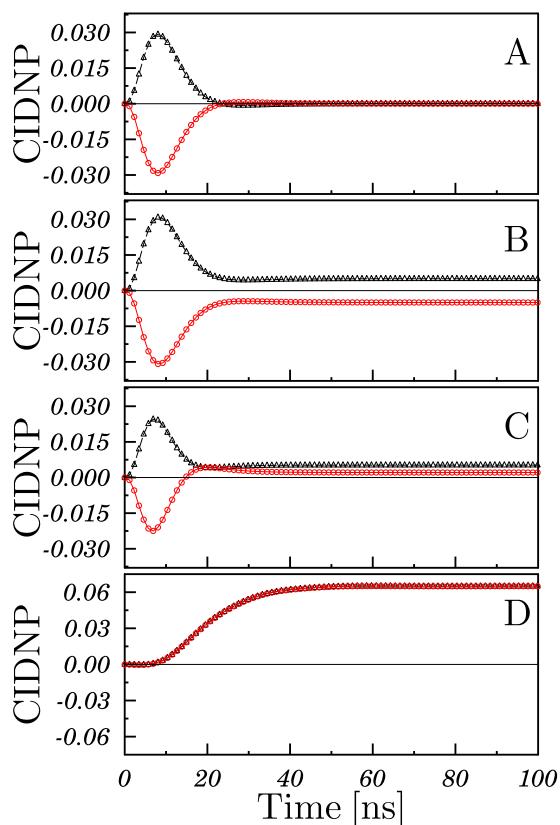


FIG. 11. Time dependence of CIDNP in an RP with two nuclei calculated for different k_S/k_T ratios. Parameters used in the calculation: $g_1=2$ and $g_2=2.0067$; the nuclei are protons; $A_1=1$ mT (black triangles); $A_2=-1$ mT (red circles). In (a) $b_1=b_2=d=0$ and the RP reaction rates are $k_S=5k_T=0.5$ ns $^{-1}$, $k_{sc}=0$; in (b) $b_1=b_2=d=0$ and $k_S=5k_T=0.5$ ns $^{-1}$, $k_{sc}=0.02$ ns $^{-1}$; in (c) $b_1=b_2=1$ mT, $d=0.5$ mT, $k_S=5k_T=0.5$ ns $^{-1}$, $k_{sc}=0.02$ ns $^{-1}$; $d=1$ mT; in (d) $b_1=b_2=1$ mT, $d=0.5$ mT, $k_S=k_T=0.1$ ns $^{-1}$, $k_{sc}=0.002$ ns $^{-1}$. The calculated CIDNP is polarization per RP.

D. ss-CIDNP field dependence

Discussion of ss-CIDNP and its field dependence is usually limited to the high-field part of the full dependence, i.e., to the case where only S- T_0 spin mixing is operating. In the corresponding field range the resulting polarization is determined by the relative efficiency of different mechanisms, i.e., by the conventional S- T_0 mixing mechanism, which is well-established in liquids and by the solid-state mechanisms discussed above. At lower fields, when the T_{\pm} levels closely approach the singlet level, the additional S- T_{\pm} mixing channels come into play. One should note, however, that “lower fields” can be quite high when the exchange coupling is strong; such examples are known, for instance, for biradicals. This is demonstrated, for instance, in Figure 7, where an additional maximum appears, coming from S- T_{-} mixing. At lower magnetic fields, i.e., when the field is comparable to HFC, additional features can appear. Here we do not analyze them in detail and only mention that they can be assigned to specific LACs in the RP spin system. Studies of the full ss-CIDNP field dependence pave the way to precise characterization of the magnetic parameters of RP; although the corresponding analysis can be relatively complicated. However, as in other cases discussed here, LACs can make such an analysis simpler. We anticipate that the same holds for more complex cases, i.e.,

for multi-nuclear RPs. In this situation, not only the electrons exhibit a more complex spin evolution but also the nuclei affect each other: although direct nuclear-nuclear interaction is very small compared, for instance, to HFC, due to coupling to the electrons CIDNP of each nucleus is sensitive to the presence of all other nuclei as well. In specific cases^{73,74} such effects can lead to violation of Kaptein’s rules in ls-CIDNP, showing that multi-nuclear RPs exhibit a complex behavior. This effect can be further complicated in solids, but we expect that the level crossing description, as proposed here, can simplify the theoretical treatment.

IV. CONCLUSIONS AND OUTLOOK

In this work we analyzed features in the magnetic field dependence of CIDNP in solids by using the idea that such features can be correlated with LCs and LACs of the spin energy of a radical pair. The validity of this concept was tested for the well understood case of ls-CIDNP; after that, we performed an analysis of ss-CIDNP.

We demonstrated that the ss-CIDNP features discussed in a number of earlier publications, see Ref. 16 for an overview, can indeed be attributed to spin mixing at particular LACs. The LAC approach to CIDNP has a number of advantages: field positions of the features and corresponding “matching conditions” become clear from the LAC analysis. Furthermore, elucidation of specific spin mixing pathways (given by the corresponding LACs) provides a relatively simple understanding of CIDNP; in particular, ss-CIDNP sign rules become clear.

For these reasons, the LC/LAC analysis opens a way to a general understanding of CIDNP in liquids and solids. Indeed, in both cases polarization is formed by the interplay of the reaction and spin dynamics; the efficiency of polarization formation increases at specific LCs and LACs, which thus define the magnetic field where different mechanisms come into play. This description also allows us to look at CIDNP from a more general perspective. Presently, each individual case in ss-CIDNP is treated separately and has a separate name (given by acronyms DD, DR, and TSM). However, these different cases are just given by different types of spin mixing in an RP, which, in turn, correspond to different LCs or LACs. While ls-CIDNP is relatively simple (for instance, the high-field CIDNP sign is described by a single rule, see Eq. (12)), the ss-CIDNP case immediately becomes complex due to anisotropic interactions and, consequently, due to a larger number of LACs. Analysis of the full ss-CIDNP field dependence would definitely reveal even further features, which all correspond to different types of spin mixing. Hence, it is not necessary to describe all types of mixing by different mechanisms; instead, we suggest assigning features to LCs and LACs and thus staying with a more general description.

While here we restricted our study to the theoretical framework the obvious test of our approach is to run field-dependent ss-CIDNP measurements over a wide magnetic field range: up to now ss-CIDNP studies were limited to the range of 1.4-17.6 T.⁷⁵ Another promising option is given by experiments on macroscopically oriented samples: in

this case, by going to different orientations it is possible to map out active LCs and LACs and determine their contribution to polarization. A candidate system for such studies is given by doped molecular single crystals such as phenazine in anthracene⁷⁶ or acridine in fluorene⁷⁷ although similar systems are normally used to generate optical nuclear polarization by a different mechanism (by transferring the electron spin polarization from a transient triplet state), also spin-correlated RPs in a triplet state can be formed, i.e., CIDNP effects can be studied. Alternatively, ss-CIDNP in membrane proteins oriented on a glass disk can be studied.⁷⁸ The utility of field-dependent ls-CIDNP studies is known for many years, in solids, such studies can provide new information about RPs and enable optimization of the polarization process. The orientation dependence of CIDNP can be exploited only in anisotropic media, i.e., in crystals, liquids crystals, etc. In general, studying orientation dependent effects in magnetic resonance is a valuable tool for probing magnetic interactions and determining molecular parameters. There is no doubt that studies of the magnetic field and orientation dependence of ss-CIDNP can provide important new insights in the mechanism of CIDNP formation and structure of RPs in solids.

Our results can be utilized to optimize CIDNP performance: by setting the external magnetic field strength in order to match a particular LC/LAC one can achieve the highest polarization. Additionally, our approach is helpful for solving the inverse problem, i.e., for determining EPR parameters of RPs by correlating features in the CIDNP field dependence with particular LACs. In this way, one can reveal the pathway of CIDNP formation (i.e., find out, which particular LC or LAC is operative), determine spin interactions in an RP (ideally, extract specific interactions from the positions of different LCs and LACs) and probe the RP reactivity (from broadening of the features in the CIDNP field dependence). Such an approach is frequently used in MARY-spectroscopy; likewise, it can provide new CIDNP insights into the spin dynamics and reactivity of RPs. Thus, our approach paves a way to an NMR based approach⁷⁹ for determining EPR parameters of elusive RPs, which are often beyond the reach of conventional EPR spectroscopy.

ACKNOWLEDGMENTS

D.V.S., H.M.V., and K.L.I. acknowledge support from the Russian Science Foundation (Grant No. 15-13-20035). All authors would like to thank the EU COST Program for allowing the successful Action No. TD1103 EuroHyperPol.

NOMENCLATURE

CIDNP	Chemically Induced Dynamics Nuclear Polarization
DD	Differential Decay
DNP	Dynamic Nuclear Polarization
DR	Differential Relaxation
EPR	Electron Paramagnetic Resonance
HFC	Hyperfine Coupling
ISC	Inter-System Crossing

LAC	Level Anti-Crossing
LC	Level Crossing
ls	liquid-state
MARY	Magnetically Affected Reaction Yield
MAS	Magic Angle Spinning
NMR	Nuclear Magnetic Resonance
RP	Radical Pair
RPM	Radical Pair Mechanism
ss	solid-state
TSM	Three Spin Mixing
ZQC	Zero-Quantum Coherence

¹K. M. Salikhov, Y. N. Molin, R. Z. Sagdeev, and A. L. Buchachenko, *Spin Polarization and Magnetic Effects in Chemical Reactions* (Elsevier, Amsterdam, 1984).

²W. B. Mims, *Phys. Rev. B* **5**, 2409 (1972).

³C. Jefferies, *Phys. Rev. B* **106**, 164 (1957).

⁴Y. Hovav, A. Feintuch, and S. Vega, *J. Magn. Reson.* **207**, 176 (2010).

⁵K.-N. Hu, H.-H. Yu, T. M. Swager, and R. G. Griffin, *J. Amer. Chem. Soc.* **126**, 10844 (2004).

⁶C. F. Hwang and D. A. Hill, *Phys. Rev. Lett.* **19**, 1011 (1967).

⁷Y. Hovav, A. Feintuch, and S. Vega, *J. Magn. Reson.* **214**, 29 (2012).

⁸P. Schosseler, T. Wacker, and A. Schweiger, *Chem. Phys. Lett.* **224**, 319 (1994).

⁹G. Jeschke and J. Matysik, *Chem. Phys.* **294**, 239 (2003).

¹⁰T. Polenova and A. E. McDermott, *J. Phys. Chem. B* **103**, 535 (1999).

¹¹A. McDermott, M. G. Zysmilich, and T. Polenova, *Solid State Nucl. Magn. Reson.* **11**, 21 (1998).

¹²G. L. Closs, *Chem. Phys. Lett.* **32**, 277 (1975).

¹³R. A. Goldstein and S. G. Boxer, *Biophys. J.* **51**, 937 (1987).

¹⁴G. Jeschke, *J. Am. Chem. Soc.* **120**, 4425 (1998).

¹⁵G. Jeschke, *J. Chem. Phys.* **106**, 10072 (1997).

¹⁶B. E. Bode, S. S. Thamarath, K. B. Sai Sankar Gupta, A. Alia, G. Jeschke, and J. Matysik, *Top. Curr. Chem.* **338**, 105 (2013).

¹⁷S. S. Thamarath, J. Heberle, P. J. Hore, T. Kottke, and J. Matysik, *J. Am. Chem. Soc.* **132**, 15542 (2010).

¹⁸I. C. Camacho and J. Matysik, in *The Biophysics of Photosynthesis*, edited by J. Golbeck and A. van der Est (Springer, 2014), p. 141.

¹⁹A. Diller, A. Alia, E. Roy, P. Gast, H. J. van Gorkom, J. Zaenen, H. J. M. de Groot, C. Glaubit, and J. Matysik, *Photosynth. Res.* **84**, 303 (2005).

²⁰W. Eisenreich, M. Joshi, S. Weber, A. Bacher, and M. Fischer, *J. Am. Chem. Soc.* **130**, 13544 (2008).

²¹G. Richter, S. Weber, W. Römisch, A. Bacher, M. Fischer, and W. Eisenreich, *J. Am. Chem. Soc.* **127**, 17245 (2005).

²²W. Eisenreich, M. Fischer, W. Römisch-Margl, M. Joshi, G. Richter, A. Bacher, and S. Weber, *Biochem. Soc. Trans.* **37**, 382 (2009).

²³G. Kothe, M. Lukaschek, G. Link, S. Kacprzak, B. Illarionov, M. Fischer, W. Eisenreich, A. Bacher, and S. Weber, *J. Phys. Chem. B* **118**, 11622 (2014).

²⁴X. Wang, S. S. Thamarath, and J. Matysik, *Acta Chim. Sin.* **71**, 169 (2013).

²⁵F. Adrian, in *Chemically Induced Dynamic Nuclear Polarization*, edited by L. T. Muus *et al.* (D. Reidel Publishing Company, Dordrecht-Holland, 1977), p. 369.

²⁶A. N. Pravdivtsev, A. V. Yurkovskaya, H.-M. Vieth, K. L. Ivanov, and R. Kaptein, *ChemPhysChem* **14**, 3327 (2013).

²⁷K. L. Ivanov, A. N. Pravdivtsev, A. V. Yurkovskaya, H.-M. Vieth, and R. Kaptein, *Prog. Nucl. Magn. Reson. Spectrosc.* **81**, 1 (2014).

²⁸A. N. Pravdivtsev, K. L. Ivanov, A. V. Yurkovskaya, P. A. Petrov, R. Kaptein, H.-H. Limbach, and H.-M. Vieth, *J. Magn. Reson.* **261**, 73 (2015).

²⁹L. Buljubasich, M. B. Franzoni, H. W. Spiess, and K. Münnemann, *J. Magn. Reson.* **219**, 33 (2012).

³⁰J. P. Colpa and D. Stehlik, *Chem. Phys.* **21**, 273 (1977).

³¹V. Macho, J. P. Colpa, and D. Stehlik, *Chem. Phys.* **44**, 113 (1979).

³²R. Fischer, C. O. Bretschneider, P. London, D. Budker, D. Gershoni, and L. Frydman, *Phys. Rev. Lett.* **111**, 057601 (2013).

³³K. R. Thurber and R. Tycko, *J. Chem. Phys.* **137**, 084508 (2012).

³⁴K. R. Thurber and R. Tycko, *Isr. J. Chem.* **54**, 39 (2014).

³⁵F. Mentink-Vigier, Ü. Akbey, Y. Hovav, S. Vega, H. Oschkinat, and A. Feintuch, *J. Magn. Reson.* **224**, 13 (2012).

³⁶R. W. Wood and A. Ellett, *Proc. R. Soc. A* **103**, 396 (1923).

³⁷W. Hanle, *Z. Phys.* **30**, 93 (1924).

- ³⁸R. A. Marcus, *Annu. Rev. Phys. Chem.* **15**, 155 (1964).
- ³⁹D. Borgis and J. T. Hynes, *Chem. Phys.* **170**, 315 (1993).
- ⁴⁰S. Hammes-Schiffer, *Acc. Chem. Res.* **34**, 273 (2001).
- ⁴¹N. J. Turro, *Modern Molecular Photochemistry* (University Science Books, Sausalito, California, 1991).
- ⁴²G. L. Closs, M. D. E. Forbes, and J. R. Norris, *J. Phys. Chem.* **91**, 3592 (1987).
- ⁴³P. J. Hore and R. W. Broadhurst, *Prog. Nucl. Magn. Reson. Spectrosc.* **25**, 345 (1993).
- ⁴⁴J.-K. Vollenweider and H. Fischer, *Chem. Phys.* **108**, 365 (1986).
- ⁴⁵J.-K. Vollenweider, H. Fischer, J. Hennig, and R. Leuschner, *Chem. Phys.* **97**, 217 (1985).
- ⁴⁶G. L. Closs and C. Doubleday, *J. Am. Chem. Soc.* **95**, 2735 (1973).
- ⁴⁷F. J. J. de Kanter, J. A. den Hollander, A. H. Huizer, and R. Kaptein, *Mol. Phys.* **34**, 857 (1977).
- ⁴⁸O. B. Morozova, Y. P. Tsentelovich, A. V. Yurkovskaya, and R. Z. Sagdeev, *J. Phys. Chem. A* **102**, 3492 (1998).
- ⁴⁹A. V. Yurkovskaya, S. Grosse, S. V. Dvinskikh, O. B. Morozova, and H.-M. Vieth, *J. Phys. Chem. A* **103**, 980 (1999).
- ⁵⁰E. D. Skakovskii, O. V. Shirokii, L. Y. Tychinskaya, M. M. Ogorodnikova, and S. V. Rykov, *J. Appl. Spectrosc.* **69**, 689 (2002).
- ⁵¹A. A. Obynochny, P. A. Purtov, A. G. Maryasov, Y. N. Molin, K. M. Salikhov, and E. D. Skakovskiy, *Appl. Magn. Reson.* **9**, 355 (1995).
- ⁵²K. Miesel, A. V. Yurkovskaya, and H.-M. Vieth, *Appl. Magn. Reson.* **26**, 51 (2004).
- ⁵³M. Wegner, H. Fischer, M. Koeberg, J. M. Verhoeven, A. M. Oliver, and M. N. Paddon-Row, *Chem. Phys.* **242**, 227 (1999).
- ⁵⁴M. Wegner, H. Fischer, S. Grosse, H.-M. Vieth, A. M. Oliver, and M. N. Paddon-Row, *Chem. Phys.* **264**, 341 (2001).
- ⁵⁵R. Kaptein, *J. Chem. Soc. D* **1971**, 732.
- ⁵⁶R. Kaptein and J. A. den Hollander, *J. Am. Chem. Soc.* **94**, 6269 (1972).
- ⁵⁷F. S. Sarvarov, K. M. Salikhov, and R. Z. Sagdeev, *Chem. Phys.* **16**, 41 (1976).
- ⁵⁸See supplementary material at <http://dx.doi.org/10.1063/1.4945341> for additional figures.
- ⁵⁹D. V. Stass, B. M. Tadjikov, and Y. N. Molin, *Chem. Phys. Lett.* **235**, 511 (1995).
- ⁶⁰V. O. Saik, A. E. Ostafin, and S. Lipsky, *J. Chem. Phys.* **103**, 7347 (1995).
- ⁶¹B. M. Tadjikov, D. V. Stass, O. M. Usov, and Y. N. Molin, *Chem. Phys. Lett.* **273**, 25 (1997).
- ⁶²O. A. Anisimov, V. M. Grigoryants, S. V. Kiyonov, K. M. Salikhov, S. A. Sukhenko, and Y. N. Molin, *Theor. Exp. Chem.* **18**, 256 (1983).
- ⁶³Y. V. Toropov, F. B. Sviridenko, D. V. Stass, A. B. Doktorov, and Y. N. Molin, *Chem. Phys.* **253**, 231 (2000).
- ⁶⁴K. L. Ivanov, N. N. Lukzen, H.-M. Vieth, S. Grosse, A. V. Yurkovskaya, and R. Z. Sagdeev, *Mol. Phys.* **100**, 1197 (2002).
- ⁶⁵K. L. Ivanov, H.-M. Vieth, K. Miesel, A. V. Yurkovskaya, and R. Z. Sagdeev, *Phys. Chem. Chem. Phys.* **5**, 3470 (2003).
- ⁶⁶D. V. Stass, N. N. Lukzen, B. M. Tadjikov, V. M. Grigoryantz, and Y. N. Molin, *Chem. Phys. Lett.* **243**, 533 (1995).
- ⁶⁷E. V. Kalneus, D. V. Stass, and Y. N. Molin, *Appl. Magn. Reson.* **28**, 213 (2005).
- ⁶⁸G. Grampp, M. Justinek, S. Landgraf, P. J. Hore, and N. N. Lukzen, *J. Am. Chem. Soc.* **126**, 5635 (2004).
- ⁶⁹K. Lüders and K. M. Salikhov, *Chem. Phys.* **117**, 113 (1987).
- ⁷⁰G. Jeschke, B. C. Anger, B. E. Bode, and J. Matysik, *J. Phys. Chem. A* **115**, 9919 (2011).
- ⁷¹G. Jeschke and A. Schweiger, *Principles of Pulse Electron Paramagnetic Resonance* (Oxford University Press, Oxford, 2001).
- ⁷²T. Maly, G. T. Debelouchina, V. S. Bajaj, K.-N. Hu, C.-G. Joo, M. L. Mak-Jurkauskas, J. R. Sirigiri, P. C. A. van der Wel, J. Herzfeld, R. J. Temkin, and R. G. Griffin, *J. Chem. Phys.* **128**, 052211 (2008).
- ⁷³K. M. Salikhov, *Chem. Phys.* **64**, 371 (1982).
- ⁷⁴P. J. Hore, S. Stob, J. Kemmink, and R. Kaptein, *Chem. Phys. Lett.* **98**, 409 (1983).
- ⁷⁵S. S. Thamarath, B. E. Bode, S. Prakash, K. B. S. S. Gupta, A. Alia, G. Jeschke, and J. Matysik, *J. Am. Chem. Soc.* **134**, 5921 (2012).
- ⁷⁶G. Dittich, D. Stehlik, and K. H. Hausser, *Z. Naturforsch., A* **32**, 652 (1977).
- ⁷⁷D. Stehlik, P. Rösch, P. Lau, H. Zimmermann, and K. H. Hausser, *Chem. Phys.* **21**, 301 (1977).
- ⁷⁸A. Diller, E. Roy, P. Gast, H. J. van Gorkom, H. J. M. de Groot, C. Glaubitz, G. Jeschke, J. Matysik, and A. Alia, *Proc. Natl. Acad. Sci. U. S. A.* **104**, 12767 (2007).
- ⁷⁹O. B. Morozova, K. L. Ivanov, A. S. Kiryutin, R. Z. Sagdeev, T. Köchling, H.-M. Vieth, and A. V. Yurkovskaya, *Phys. Chem. Chem. Phys.* **13**, 6619 (2011).